

**Coordination Chemistry in
Liquid Ammonia
and Phosphorous Donor Solvents**

Kersti B. Nilsson

Faculty of Natural Resources and Agricultural Sciences

Department of Chemistry

Uppsala

**Doctoral thesis
Swedish University of Agricultural Sciences
Uppsala 2005**

Acta Universitatis Agriculturae Sueciae

2005: number 21

ISSN 1652-6880

ISBN 91-576-7020-x

© 2005 Kersti B. Nilsson, Uppsala

Tryck: SLU Service/Repro, Uppsala 2005

Abstract

Nilsson, K. B., *Coordination chemistry in liquid ammonia and phosphorous donor solvents*.
Doctor's dissertation.
ISSN 1652-6880, ISBN 91-576-7020-x

The thesis summarizes and discusses the results from coordination chemistry studies of solvated d^{10} metal and copper(II) ions, and mercury(II) halide complexes in the strong electron-pair donor solvents liquid and aqueous ammonia, trialkyl phosphite, triphenyl phosphite and trialkylphosphine. The main techniques used are EXAFS, metal NMR and vibrational spectroscopy, and crystallography. Four crystal structures containing ammonia solvated metal ions have been determined. Questions addressed concern whether any changes in the preferential coordination numbers and geometries occur when these metal ions are transferred from aqueous ammonia to liquid ammonia solution, or to phosphorous donor solvents.

Liquid ammonia and trialkyl phosphites are found to possess similar electron-pair donor properties, $D_S=56$ for both, while trialkylphosphines are known to be even stronger electron-pair donors. The studies reveal that the ammonia-solvated d^{10} metal ions obtain very different configurations in liquid ammonia, with gold(I) being linear, copper(I) and silver(I) trigonal, zinc(II) and mercury(II) tetrahedral, and cadmium(II), indium(III) and thallium(III) octahedral. The ammonia-solvated copper(I) and silver(I) ions are linear in aqueous ammonia solution because of the lower ammonia activity, as the third ammine complexes are very weak in aqueous systems. In the phosphorous donor solvents surveyed, the copper(I) ion is tetrahedral while the silver(I) ion is tetrahedral or trigonal and the gold(I) ion is trigonal or linear.

The ammonia solvated copper(II) ion has a Jahn-Teller distorted octahedral configuration in liquid ammonia solution and solid $[\text{Cu}(\text{NH}_3)_6](\text{ClO}_4)_2$, as determined by EXAFS. In liquid ammonia, mercury(II) chloride and mercury(II) bromide are completely dissociated, whereas the ammonia solvated mercury(II) iodide, $[\text{HgI}_2(\text{NH}_3)_2]$, complex has a near tetrahedral configuration. In tri-*n*-butylphosphine, mercury(II) iodide is completely dissociated, forming a linear solvate complex in a melt at elevated temperature.

Keywords: coordination, d^{10} metal ions, copper(II), mercury(II) halides, liquid ammonia, phosphite, phosphine, solution, EXAFS.

Author's address: Kersti B. Nilsson, Department of Chemistry, P.O. Box 7015, SLU, SE-750 07, Uppsala, Sweden, kersti.nilsson@kemi.slu.se.

"The pure and simple truth is rarely pure and never simple."

--**Oscar Wilde**

Contents

Introduction	7
Ammonia	
<i>General</i>	7
<i>Properties of liquid ammonia</i>	8
Phosphorous Donor Solvents	
<i>General</i>	14
<i>Properties of phosphite and phosphine solvents</i>	15
Basic concepts	16
HSAB theory	16
The Jahn-Teller Effect (JTE)	17
The Pseudo Jahn-Teller Effect (PJTE)	18
Physical parameters important in metal NMR spectroscopy	
<i>Relaxation</i>	19
<i>Paramagnetism</i>	20
<i>Spin-spin coupling</i>	20
<i>Magnetic spin</i>	21
<i>Chemical shift</i>	22
Experimental	
Materials	
<i>Solvents</i>	22
<i>Metal ion solvate complexes</i>	23
<i>Sample holders</i>	23
Methods	24
<i>NMR Spectroscopy</i>	24
<i>Raman Spectroscopy</i>	25
<i>X-ray Diffraction in solid state (Crystallography)</i>	25
<i>X-ray Diffraction in solution (LAXS)</i>	27
<i>Extended X-ray Absorption Fine Structure (EXAFS)</i>	27
Results and discussion	
Copper(I), silver(I) and gold(I)	
<i>Ammonia solvation</i>	29
<i>Solvates of phosphites and phosphines</i>	31
<i>Relativistic effects of gold</i>	32
Copper(II)	33
Zinc(II), cadmium(II) and mercury(II)	35
Mercury(II) halides	37
Indium(III) and thallium(III)	39
Metal ion coordination in liquid ammonia and aqueous solutions	40
d^{10} Metal ion solvation in strong electron-pair donor solvents	41
Highlights	42
Future aspects	42
Acknowledgements	44
References	45
Appendices	50

Appendix

Papers I-VI

The present thesis is based on the following papers, which will be referred to by their Roman numerals:

I. Nilsson K. B. & Persson I. The coordination chemistry of copper(I) in liquid ammonia, trialkyl and triphenyl phosphite, and tri-*n*-butylphosphine solution. 2004, *Dalton Transactions*, 1312-1319.

II. Nilsson K. B., Persson I. & Kessler V.G. The coordination chemistry of the solvated silver(I) and gold(I) ions in aqueous, dimethylsulfoxide, liquid and aqueous ammonia, trialkyl and triphenyl phosphite and tri-*n*-butylphosphine solution. Submitted to *Dalton Transactions*.

III. Nilsson K. B., Persson I. & Kessler V.G. The coordination chemistry of the copper(II), zinc(II) and cadmium(II) ions in aqueous and liquid ammonia solution, and the crystal structures of hexaamminecopper(II) perchlorate and hexaamminecadmium chloride. Submitted to *Dalton Transactions*.

IV. Nilsson K. B., Maliarik M., Persson I., Fischer A., Ullström A.-S., Eriksson L., & Sandström M. The coordination chemistry of mercury(II) in aqueous and liquid ammonia solution, and the structure of tetraamminemercury(II) perchlorate in solid state. Submitted to *Dalton Transactions*.

V. Nilsson K. B., Maliarik M., Persson I., & Sandström M. Structure and solvation of mercury(II) halides in liquid ammonia, tri-*n*-butyl phosphite and tri-*n*-butylphosphine solution. (Manuscript)

VI. Nilsson K. B., Persson I. & Maliarik M. The coordination chemistry of indium(III) and thallium(III) in liquid ammonia solution. (Manuscript).

Paper I is reproduced by permission of The Royal Society of Chemistry.

Introduction

Coordination chemistry refers to the number and geometry of ligand atoms surrounding an ion in solution or solid state. The coordination geometry (including occasional distortions) of a specific metal ion is important in a number of aspects, including reactivity, electron transfer, spectrochemistry and magnetism. In a wider perspective, knowledge of the coordination preferences of a specific metal ion gives a more complete picture of coordination chemistry in general. A systematic survey of the properties of different solvents, producing a various number of coordination geometries in metal ion solvates has been accomplished during the last three decades at chemistry departments all over the world. This thesis investigates solvation of metal ions in solvents with extreme properties concerning the ability to donate electrons; liquid ammonia, trialkyl phosphites, triphenyl phosphite and trialkylphosphines. The expected coordination geometries in these systems are of low symmetry due to the dominating covalent interaction, as the orbitals available in the reacting compounds to a high extent determine the structure.

Ammonia

General

The name “*ammonia*” by origin comes from the Egyptian God Amun-Ra. Ammonia is thought to have been discovered by accident through burning the dung of camels near the temple of Ammon at the Siwa oasis in Libya. (<http://www.freemplate.ws/am/ammonia.html>; 25-Jan-2005)

The first industrial production began in 1913 in Germany. The technology was based on the Haber-Bosch process, which includes high-pressure catalytic reduction of nitrogen gas with hydrogen gas produced by electrolysis of water. (Greenwood & Earnshaw, 1997) The technology used today is essentially the same except the production of the hydrogen gas, which usually is replaced by less energy demanding processes.

Ammonia is one of the most used chemical products in the world today. The world production was 109 million tonnes in nitrogen content in the year 2003. (http://www.indexmundi.com/en/commodities/minerals/nitrogen/nitrogen_table12.html; 30-Dec-2004) In 1996 it was the single most produced chemical compound in the USA regarding the number of molecules produced. Ammonia is used primarily (>85%) as a fertilizer, where direct use is the most common, followed by composite products. Industrial uses include explosives produced by nitrates via ammonia and the production of fibres and plastic including nylon and rayon. In the household, ammonia is mainly used in detergents. Other areas include food and beverage industry, pharmaceuticals, water purification, refrigeration units and the manufacture of numerous organic and inorganic chemicals. (<http://dhfs.wisconsin.gov/eh/Air/fs/Ammonia.htm>, 15-Feb-2005)

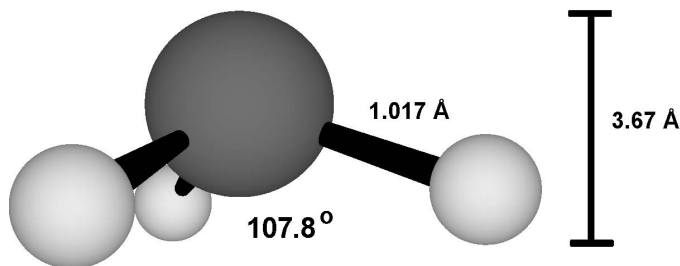


Fig. 1. The ammonia molecule, with the H-N-H angle, N-H bond distance and pyramid height displayed.

Gaseous ammonia has a unique penetrating odour, perceptible at concentrations of about 20-50 ppm. Irritation to eyes and the nasal passage begins at about 100-200 ppm and higher concentrations can be dangerous, or even lethal. (Greenwood & Earnshaw, 1997) Contact with liquid ammonia causes caustic burn and freeze burn. (<http://dhfs.wisconsin.gov/eh/Air/fs/Ammonia.htm>, 15-Feb-2005) The ammonia gas is highly soluble in water, and it is possible to dissolve it to an extent of 25% by weight in analytical grade purity and to 28% by weight in lower grade purity. The activity of ammonia determines the metal ion complex formed in aqueous ammonia.

The corrosion of copper and brass in air in the presence of ammonia is rapid, and also nickel, polyvinylchloride, and zinc are affected. (Greenwood & Earnshaw, 1997; <http://www.corrosion-doctors.org/ProcessIndustry/Process-chemicals.htm> 5-Jan-2005) Therefore it is of utmost importance that materials used when handling ammonia, such as metals and sealings, are carefully chosen.

As ammonia is an efficient nutrient source of nitrogen, the environment can be affected by nitrogen enrichment and thereby of eutrophication. The largest source of emission comes from agriculture (*e.g.* more than 80% in the UK in the year 2000). (http://www.defra.gov.uk/environment/airquality/ammonia/pdf/ammonia_summary.pdf; 19-Feb-2005) The source of ammonia emission is very diffuse and it is difficult to apply technology for its reduction. (<http://dhfs.wisconsin.gov/eh/Air/fs/Ammonia.htm>, 15-Feb-2005) The structure of ammonia is shown in Fig. 1.

Properties of liquid ammonia

In general, the properties of liquid ammonia and liquid water are quite similar. Both solvents exhibit hydrogen bonding, causing the melting points and boiling points and the heats of vaporization to be anomalously high compared with the hydrides of the other elements in the corresponding groups in the periodic table. Other notable properties are low density, low viscosity, and high permittivity.

Table 1. *Some physical properties of liquid ammonia and liquid water (at 298K or *at 239-240 K). (Burgess & Scheraga, 1976; Greenwood & Earnshaw, 1997; Jolly & Hallada; Suresh & Naik, 2000; Shipman, 1976, <http://www.nh3.org/refer/nh3ref1.html#physical%20-properties%20chart>; 2-Jan-2005)*

Property	NH ₃	H ₂ O
Melting point/K	195.4	273.2
Boiling point/K	239.7	373.2
Viscosity/10 ⁻³ ·kg ⁻¹ ·m·s ⁻¹	0.254 *	0.8903
Density/g·cm ⁻³	0.683 *	0.997
Relative permittivity	22 *	78
Heat of vaporization/kJ·mol ⁻¹	23.26	40.7
Ionization constant/mol ² ·dm ⁻²	10 ⁻³⁰ *	1.008·10 ⁻¹⁴
Hydrogen bond strength/kJ·mol ⁻¹	9.7	22.2

For comparison, some major properties of liquid ammonia and liquid water are listed in Table 1. An interesting feature is that inversion rapidly takes place when the nitrogen atom moves through the plane of the three hydrogen atoms. This affects the vibrational spectrum of the molecule and the inversion occurs in the microwave region of the spectrum at a wavelength of 1.260 cm. (Greenwood & Earnshaw, 1997)

The structures of solid and liquid ammonia

The crystal structure of solid ammonia at 171 K (Fig. 2) was reported in 1959. (Olovsson & Templeton, 1959) The coordination number of ammonia in solid state is 12, and because of the relatively weak hydrogen bonding, the structure is dominated by the packing requirements, arranged in distorted cubic close packing. The six shorter nitrogen-nitrogen distances are 3.38 Å and the six longer nitrogen-nitrogen distances are 3.96 Å. Each ammonia molecule forms 6 hydrogen bonds to 6 neighbouring nitrogen atoms. Seven other solid phases at high pressure have been identified, of which the crystal structures of four have been determined. All of the structures are close-packed or pseudo-closed-packed. (Kume, Sasaki & Shimizu, 2001)

In a comparison with solid ammonia, the structure of solid ice at atmospheric temperature and pressure is controlled by the stronger hydrogen bonds, and each oxygen is surrounded by four other oxygens in a nearly regular tetrahedral arrangement. (Greenwood & Earnshaw, 1997)

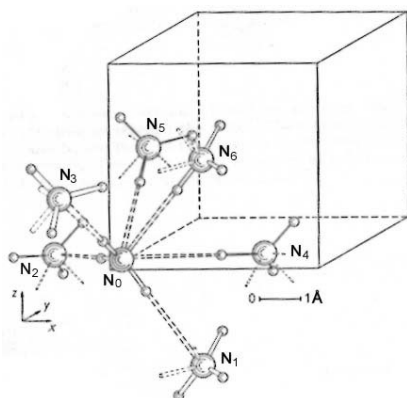


Fig. 2. The crystal structure of ammonia at 171 K.

The hydrogen bond in liquid ammonia is determined to be much weaker than the one in liquid water (Table 1). The structure of liquid ammonia is generally considered to be close packed with a coordination number of 11-14. (Kruh & Petz, 1964; Narten, 1977; Ricci, Andreani & Soper, 1995) The nitrogen-nitrogen distance is determined to be 3.4 to 3.6 Å (Kruh & Petz, 1964; Narten, 1977; Baunsenwein, Bertagnolli & David *et al.*, 1994; Ricci, Andreani & Soper, 1995), and the number of donating bonds is proposed to be less than 2 per atom, or one donating and one accepting bond. (Ricci, Andreani & Soper, 1995; Boese, Chandra & Martin *et al.*, 2003) Raman spectra were successfully interpreted with ammonia dimer as a representative of ammonia clusters. The amount of dimers increases with decreasing temperature, as the hydrogen bonding becomes more extensive at lower temperatures. (Ujike & Tominaga, 2002)

One can further compare the structure of liquid ammonia with the structure of liquid water, which has been extensively surveyed during more than 70 years, and has resulted in controversial models. The structure was recently reinvestigated, using XAS and X-ray Raman scattering compared with computed theoretical spectra, and it was concluded that each water molecule has on average 2.2 ± 0.5 hydrogen bonds (one donating and one accepting). The structure (Fig. 3) was interpreted as water molecules present in hydrogen bonded chains or rings in a distorted cluster network, not arranged as in bulk ice, thus more similar to the structure of liquid ammonia than to the structure of ice. (Wernet, Nordlund & Bergman *et al.*, 2004) The similarity of the hydrogen bonding situation in liquid water and liquid ammonia was also concluded by determination of a deuterium quadrupole coupling constant in liquid ammonia, using NMR. (Hardy & Zeidler, 2000)

The coordination structure of the hydrated proton, isostructural to ammonia, has been determined to a distorted tetrahedral configuration with one hydrogen bond significantly longer (2.90 Å) and three shorter (2.44 Å). (Lee, Matsumoto & Yamaguchi *et al.*, 1983) The result implying a distorted configuration has been supported by LAXS results, but with short hydrogen bond distances of 2.74-2.76 Å, and with a second hydration sphere of six water molecules, with an average O...O distance between the spheres of 2.76 Å. (Smiechowski & Persson) In the coordination of the hydrated proton, as well as in water coordination in ice, the

hydrogen bonds rule the structure. In both liquid and solid ammonia, the weaker hydrogen bonds govern the structure to a much lesser extent.

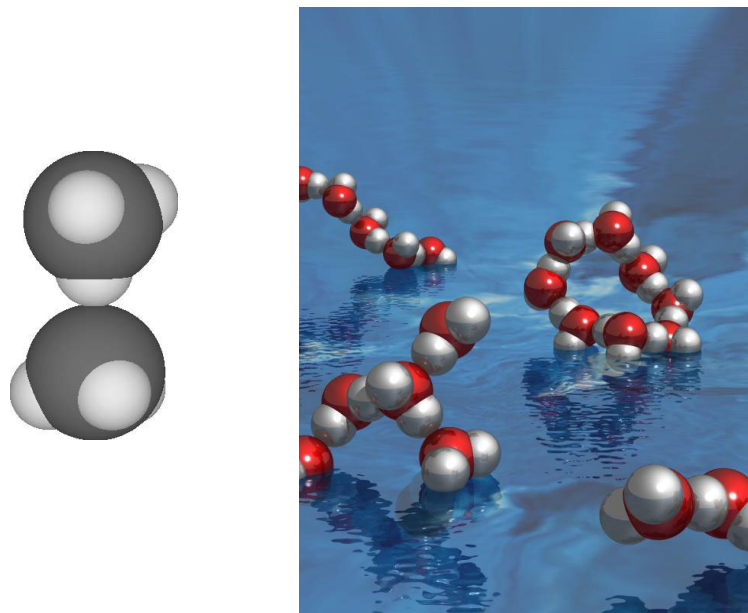


Fig 3. The hydrogen bonded ammonia dimer (left) and a picture of liquid water (right; Artwork by H. Ogasawara).

The ionization constant of ammonia is much lower than the one of water, (Table 1) but NH_4^+ and NH_2^- do exist in liquid ammonia. Any migration of protonic defects is not considered to occur in liquid ammonia, as it does in liquid water. (Liu & Tuckerman, 2001) In liquid water, the structural diffusion is thought to take place via a Grotthus type structural diffusion, a sequence of "proton hops". The mechanism behind the proton mobility is not fully elucidated, but it is thought that the limiting process is the cleavage of a second shell hydrogen bond. (Agmon, 1995) The lack of proton transport in the case of the ammonium ion is proposed to be caused by the very large discrepancy between the coordination sphere of the ammonium ion with a coordination number of 4 and ammonia with a coordination number of 11-14, (Kruh & Petz, 1964; Narten, 1977; Ricci, Andreani & Soper, 1995) complicating a second shell hydrogen bond cleavage.

Concerning the amide ion, the coordination number is 7-8 with about half of the neighbours hydrogen bonded. This is slightly closer to the coordination number of ammonia. Only accepting hydrogen bonds on the amide nitrogen are thought to exist, but for the diffusion process there is a requirement of donating hydrogens on the amide ion to promote proton transport. This is assumed as a likely explanation in addition to the discrepancies in coordination number, to be the reason for the lack of proton mediated structural diffusion also for the amide ion. (Liu & Tuckerman, 2001)

Liquid ammonia as a solvent

Liquid ammonia is the most studied electrolyte non-aqueous solvent and exhibits many interesting properties, the most conspicuous one being the ability of producing solvated electrons. This feature was first discovered by Sir Humphry Davy in 1808 (unpublished) (Greenwood & Earnshaw, 1997) and the metal-ammonia solutions have been extensively studied. Alkali metals are easily dissolved in liquid ammonia, and at low metal concentrations a deep blue coloured solution, paramagnetic with high conductivity is formed. When the metal concentration increases, the conductivity decreases and the solution becomes diamagnetic. If the metal concentration is further increased, a metallic bronze-coloured and weakly paramagnetic solution with very high conductivity is formed, approaching values typical of liquid metals. The properties in the dilute solution are caused by ionized alkali metals producing ammonia solvated electrons. The solvated electron has a broad absorption band at ca 1500 nm, and the short wavelength tail is the origin of the deep-blue colour of the solutions. The electrons are located in cavities in the solvent, and the density of the solution is much lower than the one of pure liquid ammonia. (Greenwood & Earnshaw, 1997) The hydrogen bonding is severely disrupted by the addition of metal, and completely absent at saturation. Percolation channels are formed in the metallic-liquid ammonia solutions where the electrons can be transported, and this causes the high conductivity and low density. (Thompson, Wasse & Skipper *et al.*, 2003)

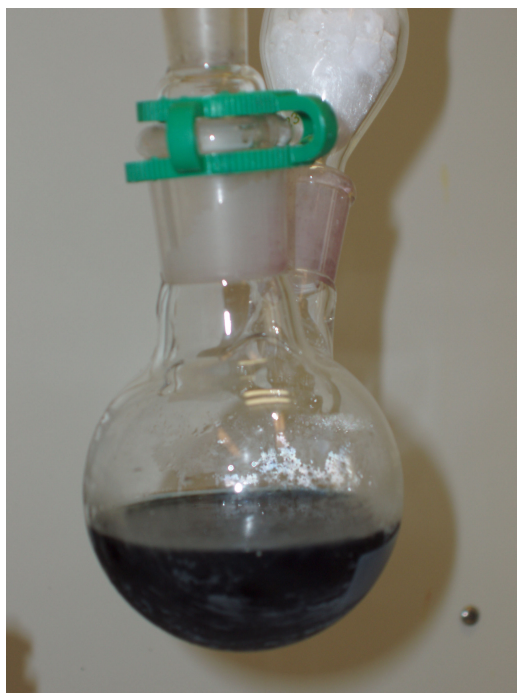


Fig. 4. A liquid ammonia solution containing ammonia solvated electrons, produced from sodium.

Also the metals calcium, strontium, barium, europium and ytterbium have been discovered to produce metal-ammonia solutions. The limit of metal solubility in liquid ammonia is linked to the standard electrode potential, which must be less

than -3 V, which excludes all of the metals used in this work. In short, low ionization energies and high cation solvation energy promotes solubility. Fig. 4 shows the appearance of ammonia solvated electrons produced from sodium dissolved in liquid ammonia.

An important use of alkali metal liquid ammonia solutions is the preparation of versatile reducing agents, carrying out reactions with organic compounds that otherwise are difficult or impossible to perform. Liquid ammonia is also possible to use for the preparation of compounds of elements with unusually low oxidation states, such as nickel(0), nickel(I), palladium(0), platinum(0), cobalt(0) and cobalt(I). (Greenwood & Earnshaw, 1997)

In other respects than alkali or rare earth metal solvation, the reactions taking place in liquid ammonia are usually in analogy with the ones occurring in water. Ammonia is the most frequently examined ligand in studies of complex formation in water and the formation of the bisamminesilver(I) complex in water was studied as early as in 1899, followed by the bisamminecopper(I) complex in 1901, the tetraamminezinc(II) and hexaamminecadmium(II) complexes in 1903 and the tetraamminenickel(II) complex in 1904. (IUPAC, 2000)

Studies of solvation and complex formation of metal ions in liquid ammonia were performed in the 1970's mainly using vibration spectroscopy. (Gans & Gill, 1976) EXAFS spectroscopic studies have also been applied in the study of ammonia solvated metal ions such as silver(I) and copper(II) ions in liquid ammonia. (Yamaguchi, Wakita & Nomura, 1988; Valli, Matsuo & Wakita *et al.*, 1996)

In this thesis only metal ion solvation with common chemical bonding properties is expected, without any formation of solvated electrons. However, the difference from hydration is important. The donating atom in liquid ammonia is nitrogen instead of the highly electronegative oxygen in water, and according to the HSAB concept, (p. 16) the electron-pair donor properties of liquid ammonia are much different from those of water. This fact implies that a specific "soft" or "hard" metal ion (p. 16) is likely to be strongly solvated in either of these two solvents.

Liquid two-phase systems

When an alkali or rare earth metal, such as sodium, is gradually added to a liquid ammonia solution (or the other way around), a liquid-liquid phase separated system can be formed. The immiscibility was discovered by Kraus in 1907, (Kraus, 1908) and the feature has been observed for Li, Na, K, Rb, Ca, Sr and Ba. (Jolly, 1959; Wasse, Hayama & Skipper *et al.*, 2003) The systems consist of two immiscible liquid phases containing the same metal at equilibrium, a bright blue dense phase and a lighter, metal-like bronze-coloured phase. Both of them are extremely good conductors of electricity. The blue colour in the denser phase is due to ammonia solvated electrons as in the metal-ammonia solutions described above. This phase is less concentrated in metal than the lighter phase, in which fully delocalized electrons are transported in cavities (causing the low density) between $M(NH_3)_n$ species. (Jolly, 1959, 1991) The cavities can be formed due to

the strongly solvated cations in the metal-like phase. (Thompson, Wasse & Skipper *et al.*, 2003)

The immiscibility gap occurs at certain low temperatures and in certain ammonia-to-metal ratios. In the case of sodium the temperature is between ca -40 and -80 °C and the metal concentration is 2-10 atom%. (Jolly, 1991) The phase diagram of the extensively studied lithium-ammonia system is more complex, and there is evidence of three different phases of $\text{Li}(\text{NH}_3)_4$. (Jolly, 1959) All alkali metals except cesium have been shown to produce immiscibility gaps. (Jolly, 1991) As the cesium-nitrogen mean bond distance is longer (2.9-3.5 Å) than the M-N bond distances present in liquid-liquid phase separated solutions, it is probable that the cavities important to the formation of a light phase are not produced with this metal. (Thompson, 1976) One of the recently examined liquid two-phase systems is the one produced from rubidium metal, studied by EXAFS technique, and the Rb-N mean bond distance was determined to 2.85 Å. (Thompson, Wasse & Skipper *et al.*, 2003) So far, no phase-phase separation in liquid ammonia formed from an originally oxidized metal ion has been described.

Phosphorous donor solvents

General

Alkyl phosphites are versatile reagents in industrial applications, including preparation of vinyl phosphate, insecticides, manufacture of lubricant additives, synthesis of flame retardants, dyes, plasticizers and other modifiers of plastics and resins, and synthesis of pharmaceuticals. Alkyl phosphites are used in the manufacture of G-type nerve agents. They can be produced by the reaction of phosphorus trichloride and an alcohol. (<http://www.cbwinfo.com/Chemical/Precursors/Phosphites.html>; 7-Dec-2004)

Phosphines are alkyl or aryl substituted phosphorous atoms, while phosphites are substituted oxidized phosphorous atoms. The substituents used in this work are methyl, ethyl, isopropyl, *n*-butyl and phenyl. Two of the structures are displayed in Fig. 5.

Trimethyl and triethyl phosphites are harmful irritants. They can cause irritation to the eye, skin and lungs. At high concentrations, irritation of the lungs can cause oedema. Chronic exposure may lead to long-term problems including emphysema and liver and kidney damage. There is evidence that they are carcinogenic and teratogenic.

Triphenylphosphine is used in organic synthesis, phosphonium salts, other phosphorous compounds and as a polymerisation initiator. (http://www.alkalimetals.com/specs/tri_phenyl_phosphine_specs.html; 9-Dec-2004)

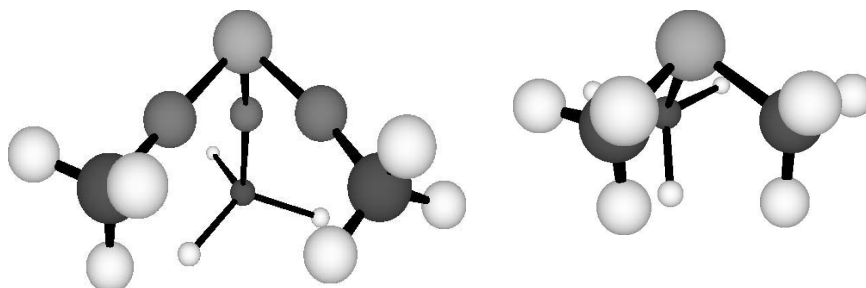


Fig. 5. Trimethyl phosphite (left) and trimethylphosphine (right).

Properties of phosphite and phosphine solvents

Trimethyl phosphite is a colorless, flammable liquid emitting a distinctive, pungent, pyridine-like odour. An odour threshold of 0.0001 ppm in air has been reported. Toxic gases (such as oxides of phosphorus) may be released in case of fire involving trimethyl phosphite. It is insoluble in water (hydrolyzes to form dimethyl phosphite and methanol) and miscible with alcohol, acetone, ether, benzene and most common organic solvents. (<http://www.osha.gov/SLTC/health-guidelines/trimethylphosphite/>; 7-Dec-2004) Selected properties are shown in Table 2.

A feature of the phosphite and phosphine solvents is the bulkiness, sometimes affecting the coordination geometries of complexes (Paper I). The bulkiness of these phosphorous donor solvents has been estimated as the “ligand cone angles”. (Tolman, 1977) The cone angle of a ligand is the steric parameter, θ , for symmetric ligands (all three substituents are the same). θ is the apex angle of a cylindrical cone formed by the organic substituents, centred 2.28 Å from the phosphorous atom. This angle just touches the van der Waals radii of the outermost atoms of a physical model of the different phosphite and phosphine ligands. The available ligand cone angles of the phosphites and phosphines, applied in Papers I, II and V, are tabulated in Appendix B.

Table 2. *Some selected physical properties of trimethyl phosphite and trimethylphosphine.* (<http://www.osha.gov/SLTC/healthguidelines/trimethylphosphite/>; 7-Dec-2004; <http://www.alfa.com>; 2-Jan-2005)

Property	Trimethyl phosphite	Trimethylphosphine
Melting point/K	195	187
Boiling point/K	384	311-312
Density(298 K)/g·cm ⁻¹	1.046	0.735

Basic concepts

In the following section some selected fundamental principles are presented. These are important for the choice of methods and for a general comprehension of the presented results.

HSAB theory

In an attempt to systematize the stabilities of different metal ion complexes, a partition of metal ions into “class a” and “class b” metal ions was suggested, based on the strength of complexes formed with a donor atom in the series F, Cl, Br, I. (Ahrland, Chatt & Davies, 1958) This approach was later developed to comprise both metal ions and ligands and the concept of “Hard” and “Soft” (Lewis) “Acids” (metal ions and hydrogen) and (Lewis) “Bases” (ligands) was introduced. (Pearson, 1963) “*Hard Acids prefer to bind to Hard Bases and Soft Acids prefer to bind to Soft Bases*”, which is basically a pragmatic and qualitative rule. In principle, “class a” or “hard” stands for metal ions or ligands establishing mainly electrostatic interactions with weak electron-pair donor properties and “class b” or “soft” stands for metal ions or ligands forming mainly covalent interactions with strong electron-pair donor properties. “Hard” metal ions are small and possess high charge density (examples are Ti(IV) and Al(III)) and thereby gaining the highest electrostatic interactions possible. Their HOMO-LUMO (Highest Occupied Molecular Orbital-Lowest Unoccupied Molecular Orbital) gap is large, providing better possibilities for electrostatic attraction. “Hard” ligands are similarly small and with highly electronegative donor atoms such as fluorine and oxygen.

“Soft” metal ions have low charge density, possess many *d*-electrons, are large, and thereby they have the greatest possibilities of being polarized. Their HOMO-LUMO gap is small with better possibilities of mixing with the ground states. The softest one is the d^{10} gold(I) ion. (Huheey, Keiter & Keiter, 1993) In “soft” ligands, the donor atoms possess low electronegativity, as in phosphorous, sulphur and iodine. Of the metal ions investigated in this thesis, all except copper(II) and cadmium(II) (both intermediate) and indium(III) (hard) are regarded as soft. (Pearson, 1963) The classification of the zinc(II) ion is not straightforward, as it behaves as a “hard” or “soft” ion depending on the properties of the solvent applied.

Several scales for classification of the electron-pair donor abilities of solvents have been constructed. The best known is the D_N scale, based on calorimetric measurements and expressed by the heat of reaction of $\text{SbCl}_5 + \text{L} \rightarrow \text{SbCl}_5\text{L}$ in benzene solution. (Gutmann & Wychera, 1966) The most relevant one in the context of strong electron-pair donors is the D_S scale, (Sandström, Persson & Persson, 1990) as it takes more of soft ligand properties into consideration. This scale is constructed as the difference between the symmetric stretching vibration, $\nu_1(\text{Hg-Br})$, of mercury(II) bromide in the gaseous phase and the investigated solvent.

$$D_S = \nu_{\text{HgBr}_2(\text{g})} - \nu_{\text{HgBr}_2(\text{solv.})}$$

In text books, *i.e.* (Huheey, Keiter & Keiter, 1993) ammonia and amines are usually regarded as “hard”, but on the D_S scale, liquid ammonia is regarded as a very strong electron-pair donor solvent with a value of 56. Tri-*n*-butyl phosphite and tri-*n*-butylphosphine are also regarded as very strong electron donor solvents with D_S values of 56 and 76, respectively.

The Jahn-Teller Effect (JTE)

A theorem proposed by H. A. Jahn and E. Teller in 1937, (Jahn & Teller, 1937) states that a molecule in a degenerate electronic state will be unstable and will undergo a geometrical distortion that lowers its symmetry and splits the degenerate state. In the literature these distortions have been regarded as especially important and are well documented for octahedrally coordinated metal ions whose e_g (*i.e.* axial) orbitals are unequally occupied. Of the metals included in the thesis, the copper(II) ion (Paper III) with $t_{2g}^6 e_g^3$ configuration is subject to this effect. (Greenwood & Earnshaw, 1997; Persson, Persson & Sandström *et al.*, 2002) The approach is not at all restricted to any special type of molecular polyatomic system, but can be used as a tool for solving theoretical molecular and crystal problems in any system with two or more atoms. (Bersuker, 2001) It is especially important when there are two or more coinciding (degenerate) electronic states (ground or excited) that become sufficiently strongly mixed when the nuclei displace from their initial reference configuration. In Fig. 6, the principle of octahedral distortion is depicted.

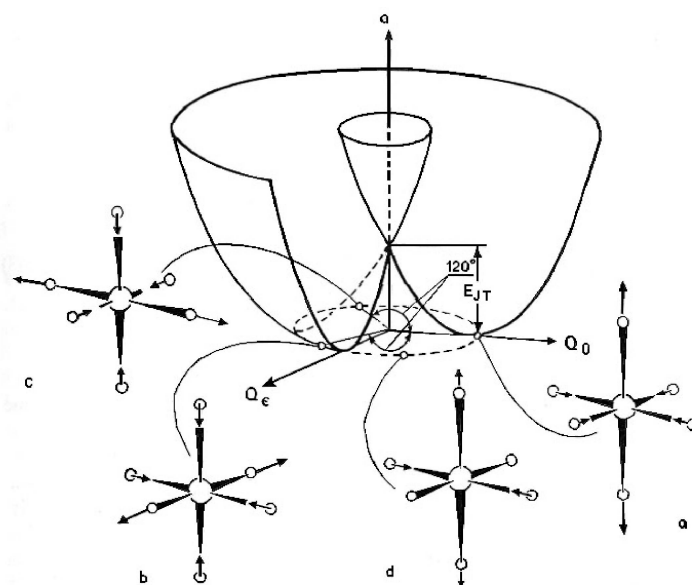


Fig. 6. APES shape and distortions of an octahedral system ML_6 at different points along the energy minima of the “Mexican hat”. (Figure reproduced from (Bersuker, 1996) © 1996 by John Wiley & Sons, Inc, reprinted with permission of John Wiley & Sons, Inc.)

The JT (and/or PJTE) vibronic coupling effects could also be regarded to trigger a symmetry breaking in a molecular system, and thereby changing it into a lower symmetry. (Bersuker, 2001) A temperature-dependent symmetry breaking takes place for instance when solid hexaamminecopper(II) perchlorate, structurally determined to a cubic space group, is cooled to 147 K (Paper III). At this point a phase transition occurs, and the symmetry of the crystal is broken to a lower one, the new phase reflecting the coordination symmetry of each copper(II) ion.

The Pseudo Jahn-Teller Effect (PJTE)

The pseudo-Jahn-Teller effect (PJTE) is equal to the Jahn-Teller theorem but applied on vibronic coupling of two (or more) excited electronic states not coinciding, but close enough to mix (pseudo-degenerate) when their nuclei displace from their original positions. These two effects are described by two different and independent vibronic coupling constants. The PJTE can be very strong when the JTE is zero, since a large vibronic coupling constant and/or a small force constant could also produce a large effect. (Bersuker, 2001) The PJTE is most pronounced in compounds where the proportion of covalent bonding is large and the HOMO-LUMO gap is small, (Bersuker, 1996) as for example in solvates of liquid ammonia and phosphine. With this theory included, there are no exceptions from the vibronic coupling effects. JTE allows for even distortions only (no dipole created), while PJTE can produce both even and odd distortions. The difference in potentials between JTE and PJTE is shown in Fig. 7. A solvated ion included in the thesis, subject to the PJTE is the tetraamminemercury(II) ion (Paper IV).

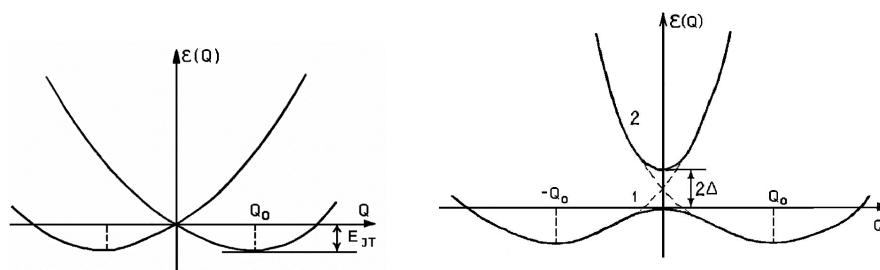


Fig. 7. Left: variation of the adiabatic potential of a molecular system in a twofold orbitally degenerate electronic state with respect to one active coordinate Q . E_{JT} is the Jahn-Teller stabilization energy. Right: A system with two sufficiently close energy levels that mix under the Q displacements. (Figure reproduced from (Bersuker, 1996) © 1996 by John Wiley & Sons, Inc, reprinted with permission of John Wiley & Sons, Inc.)

Physical parameters important in metal NMR spectroscopy

Relaxation

When a sample is placed in a strong magnetic field, the present nuclei possessing spin generate a bulk macroscopic magnetization. The magnetization of the system can be perturbed by a pulse of radio frequency, and the response of the nuclei in the system can be measured as a function of time. A certain amount of energy will affect the nucleus and change the direction of the magnetic spinning around its own axis. When there is no more energy supplied, the nucleus will go back to its equilibrium. This process is called relaxation and when heavy atom spin $I=1/2$ nuclei are involved, it consists of four different mechanisms. The time constant, describing the process when the nucleus is retaining equilibrium along the Z-axis, is called the spin-lattice or longitudinal relaxation time constant (T_1). The relaxation time constants are different for different nuclei, and also differ with the coordination geometry and the kind of atoms surrounding a specific nucleus. In addition to T_1 , there is also the spin-spin or transverse relaxation time constant (T_2). T_2 may be smaller than T_1 , but can never be larger than T_1 . If T_2 is short, the line width of the signal is broad.

The spin-lattice relaxation rates of heavy atom spin $I=1/2$ nuclei are determined from a combination of relaxation mechanisms; the nuclear dipole-dipole (DD) interaction between the heavy atom nucleus and other magnetic nuclei present in solution, the anisotropic chemical shielding (CSA) interactions, the spin-rotation (SR) interactions and the scalar coupling (SC) between the heavy atom nucleus and the magnetic nuclei in its inner coordination shell. The relaxation rates ($1/T_1$) are assumed to be additive. Also paramagnetic impurities contribute to the spin-lattice relaxation rate. Contributions from the different relaxation mechanisms can be determined and if the T_1 relaxation rate is dominated by the anisotropic chemical shielding interactions (CSA), relaxation rate determinations can be used to probe the local environment around the nucleus. Thereby, structural information about the investigated complex can be obtained. (Paper IV). The relaxation time (T_1) can be derived from the expression:

$$M_Z = M_0 (1 - e^{-t/T_1}),$$

Where M_Z is the longitudinal magnetization,
 M_0 is the equilibrium magnetization and
 t is the applied variable time delay in the inversion-recovery sequence,
used to measure T_1 .

In order to distinguish the dominating mechanisms, the dependence of the relaxation rate on magnetic field and temperature can be studied. The role of the DD relaxation can be evaluated using *e.g.* isotope substitution, and the CSA contribution increases with the square of the magnetic field. In the case of the DD and the CSA mechanisms, the only temperature dependent variable is the rotation correlation time, τ_c , which generally decreases with increasing temperature. Because of an inverse proportionality of τ_1 (angular momentum correlation time; a variable in SR interactions) to τ_c , the SR mechanism introduces an opposite

temperature dependence (more efficient at higher temperatures). Finally, for the SC interactions to be efficient, the Larmor frequencies of the interacting nuclei must be close to each other, which is rare. (Howarth, 1987; Wasylishen, 1987; Bodor, Bányai & Kowalewski *et al.*, 2002)

The relaxation process also affects the possibilities of utilizing different nuclei in NMR spectroscopy. For instance, relaxation times for ^{107}Ag and ^{109}Ag (Paper II) of more than 15 minutes have been determined. (Gill, Rodehüser & Rubini *et al.*, 1990) The effect is very time consuming NMR analyses, and together with the low receptivity of the silver nuclei restricts the use of NMR as a tool for determining structural parameters.

Paramagnetism

Diamagnetic nuclei with anti-parallel spins are only slightly affected by a magnetic field and are more easily subject to NMR analysis than paramagnetic nuclei with parallel spins. As paramagnetic impurities contribute to the spin-lattice relaxation rate, they can affect the analysis of diamagnetic nuclei. An example is in ^{63}Cu NMR, where the presence of paramagnetic copper(II) extensively broadens the line widths of the signals (Paper I). As it affects relaxation times, paramagnetic impurities possibly reduces an unfavourable T_1/T_2 ratio and thereby shortens the NMR measuring time of *i.e.* silver(I) compounds. (Borges, Koschmieder & Sahn *et al.*, 1973)

Spin-spin coupling

A very important piece of information is given by the spin-spin coupling to atoms surrounding the investigated nucleus. The spin state energy levels of the nucleus are split by other magnetic fields, induced by nuclei in the neighbouring environment. The strength of the interaction is expressed by the coupling constant, J , measured in Hz. The coupling pattern can often be interpreted, and generally the splitting caused by a nucleus with spin $I=n$ results in $2n + 1$ lines. (Paper I) One of the consequences with the lack of electron transport in liquid ammonia (p. 11) is that when applying ^1H and ^{14}N NMR on liquid ammonia solutions, only extremely dry samples will show ^1H - ^{14}N -coupling.

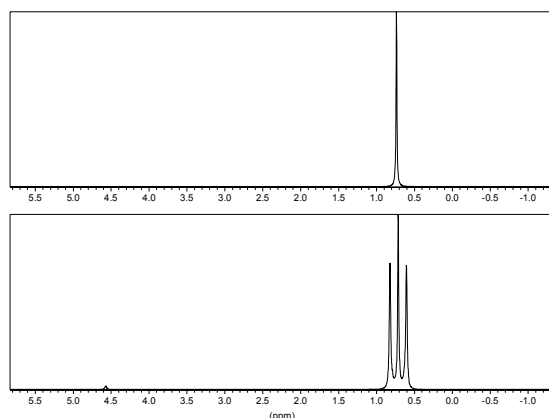


Fig. 9a. ^1H NMR spectra of the utilized (top) and extremely dry (bottom) liquid ammonia.

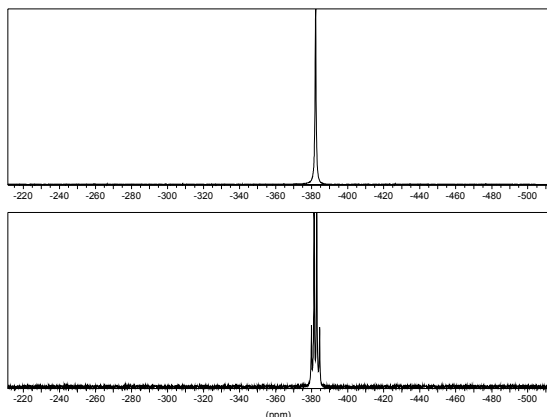


Fig. 9b. ^{14}N NMR spectra of the utilized (top) and extremely dry (bottom) liquid ammonia.

In the sodium hydroxide dried solutions it is possible to observe both a quartet from ^1H - ^{14}N -coupling in the ^{14}N NMR spectrum and a triplet from ^{14}N - ^1H -coupling in the ^1H NMR spectrum, (Figs. 9a and b) while in the utilized liquid ammonia solutions a single average signal is observed.

The time scale in NMR measurements is sometimes too long compared with ligand exchange rates in a complex to be able to see coupling between the atoms in a complex, as in ^{107}Ag and ^{199}Hg NMR. The time average of the different complexes contributing to the NMR signal will be detected, resulting in a single resonance line (Papers II and IV).

Magnetic spin

A fundamental property of the nucleus is the spin. Nuclei with spin $I=0$ are composed of an even number of protons and neutrons and have no magnetic moment. Nuclei with spin $I=1/2$ are usually simple to apply, but there are also possibilities of analysing nuclei with spin $I>1/2$. One property of the latter nuclei, complicating NMR analyses is the quadrupole moment due to non-spherical spinning charges. This property can be compared with the well-known dipole moment, where a molecule has a charge distribution with one positive and one negative part. In a quadrupole, the charge is distributed into four parts of the molecule. The effects can be seen in ^{63}Cu ($I=3/2$) NMR spectroscopy, where only highly symmetric cubic or octahedral complexes can be detected (Fig. 10 and Paper I). In the case of non-spherical charge distribution, the line widths of the signals will be strongly broadened and sometimes even beyond detection. Thereby the applicability of the method is restricted only to a limited number of copper(I) complexes.

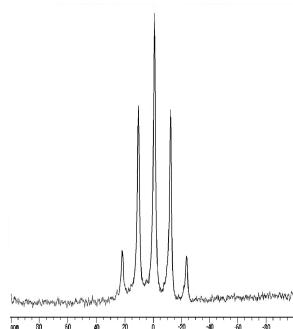
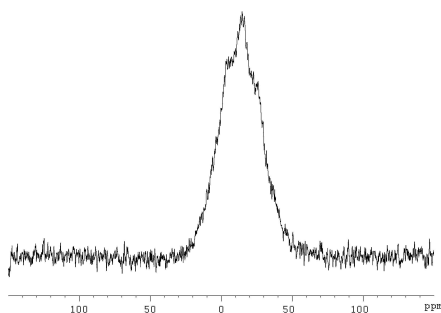


Fig. 10. ^{63}Cu NMR spectra of solutions of a highly symmetric compound, $\text{Cu}[\text{P}(\text{OC}_2\text{H}_5)_3]_4^+$ (top) and a less symmetric one, $\text{Cu}[\text{P}(\text{OCH}(\text{CH}_3)_2)_3]_4^+$ (bottom).



Chemical shift

The chemical shift is a principal parameter in NMR spectroscopy. The chemical environment causes a shielding of the nucleus from the magnetic field by the surrounding nuclei, and makes the signal to go downfield if the shielding is larger relative to a reference compound and upfield if the shielding is smaller (deshielding as a result of an enhanced magnetic field) relative to the reference compound. The shift provides information about the local magnetic field around the nucleus, and varies accordingly to the types of nuclei and bonds in the molecule. The range of shifts is very different for different nuclei. For ^1H the range is ca 15 ppm, and for ^{199}Hg the range is about 4000 ppm. The shift of a nucleus may also provide information about the coordination sphere of a metal ion, *i.e.* tetrahedral and octahedral mercury(II) complexes (Paper IV).

Experimental

Materials

Solvents

Liquid ammonia solutions were distilled from 25% aqueous ammonia (Analytical grade, Merck) and used within a few hours. Attempts were made to use liquid ammonia from gas cylinders, but the purity of the solvent produced this way was not satisfactory, since gaseous ammonia is highly corrosive to metals. The

distillation was performed by carefully heating the aqueous ammonia, letting the ammonia gas pass a glass tube filled with sodium hydroxide pastilles, and then trapping the liquid ammonia onto a "cold finger" filled with ethanol and solid carbon dioxide. The liquid ammonia was kept in a flask chilled as above in a Dewar vessel at a temperature of about 220 K. In order to avoid the presence of water, vessels containing gaseous or liquid ammonia were connected to tubes filled with solid sodium hydroxide pastilles before contact with air. For the study of solvated electrons, in metal-ammonia solutions there are requirements of inert atmosphere and of extreme purity regarding solutions and metals as well as the containers, in order to keep the solutions from decomposing. (Thompson, 1976) These cleaning processes, including reaction of sodium metal with present water in the liquid ammonia solution, multiple distillations and removing of dissolved hydrogen, were not regarded as necessary for the study of metal ion solvation in liquid ammonia. The aqueous ammonia and phosphorous donor solvents were used as purchased.

Metal ion solvate complexes

The copper(I) compounds were made from *tetrakis(acetonitrile)copper(I) perchlorate*, $[\text{Cu}(\text{CH}_3\text{CN})_4]\text{ClO}_4$, prepared as described elsewhere (Hemmerich & Sigwart, 1963) and gold(I) compounds were made from solid *bisamminegold(I) tetrafluoroborate*, $[\text{Au}(\text{NH}_3)_2]\text{BF}_4$, prepared as described in Paper II. Solid compounds and solutions containing other metal ions have generally been prepared by dissolving a perchlorate, trifluoromethanesulfonate or chloride salt in freshly distilled liquid ammonia solution. When the temperature of the cooling bath has been gradually increasing due to sublimation of the solid carbon dioxide, the liquid ammonia has relatively slowly boiled off and crystals formed. In many cases the crystals were sensitive to room temperature and/or daylight, and therefore stored in a refrigerated dry place prior to analysis, or analysed immediately after the preparation. In order to keep the copper(I) ions stable in liquid ammonia solution, hydrazine, (Aldrich), 1.25%(vol.), was added in order to reduce any copper(II) formed through air-oxidation back to copper(I) by oxidation of hydrazine to N_2 . The solutions of tetrakis(trimethylphosphite)copper(I) and tetrakis(triethylphosphite)copper(I) perchlorate in chloroform are sensitive to air-oxidation. These solutions were therefore prepared in nitrogen atmosphere, in a glove box, and transferred into argon filled NMR tubes. (Paper I)

Sample holders

In general, the equipment used for EXAFS measurements on metal ion-ammonia solutions consisted of a 2 mm titanium spacer covered with 35-55 μm glass windows and equipped with a copper rod, which was dipped into a cooling mixture made of methanol/liquid nitrogen, keeping a temperature of ca. 175 K. The temperature slowly increased during the experiment due to evaporation of the liquid nitrogen. In order to avoid ice formation, the sample cell was placed into a Perspex[®] box (50x50x50 mm) filled with nitrogen gas, enclosing the cell windows made of 6 μm X-ray propylene film. The box was equipped with a gasket sealed 8 mm aperture. A picture of the equipment is presented in Fig. 11. When the energy

of the K-edge was sufficiently high, as for silver, cadmium and indium, an ordinary 1.5 ml glass vial, equipped with an air-tight teflon/PTFE sealed cap, was used as a sample cell.



Fig. 11. Equipment used for measurement of X-ray absorption in the EXAFS experiments. (Photo: Magnus Sandström)

Methods

Nearly all of the techniques applied in the thesis are spectroscopic methods. X-ray diffraction technique is the exception, even if the energy source originates from electromagnetic radiation. Spectroscopic methods use electromagnetic radiation to investigate the interactions of specific wavelengths and quantized energy states of matter. By using various methods, different properties of the investigated compounds can be evaluated. The wavelengths of X-ray emission correspond to interatomic distances and consequently these methods are very powerful in structure determination. Going from longer to shorter wavelengths (lower to higher energy), a short description of the methods, what they actually measure and the information they provide will follow. It is of great importance not to rely on one single method, but to use methods working with completely different physical principles in order to draw the right conclusions from information achieved.

NMR Spectroscopy

The NMR instruments require strong external magnetic fields; the ones used are of 7.1 T (Bruker AMX300), 9.4 T (Bruker DRX400) and 11.7 T (Bruker AMX500). The pulsed energy corresponding to a change of the nuclear spin is of ca 10 m (radio) wavelength. The phenomenon of nuclear resonance was first observed in

1946 by two teams of physicists; Purcell, Torrey and Pound at Harvard and Bloch, Hansen and Packard at Stanford. Purcell and Bloch shared the 1952 Nobel Prize for the discovery. The structural information provided is more thoroughly presented in the chapter “Physical parameters important in NMR spectroscopy” on page 19. The ^{63}Cu , ^{107}Ag and ^{199}Hg NMR spectra were recorded on the Bruker DRX400 spectrometer equipped with a multinuclear BBO probe, at 106.05, 16.20 and 71.33 MHz, respectively. The inner diameter of the probe was 5 mm. A more complete physical background of NMR spectroscopy can be found elsewhere. (Sanders & Hunter, 1993)

Raman Spectroscopy

In Raman spectroscopy, the wavelength corresponds to vibrations within a molecule and emanates from differences between ground state vibrational and excited vibrational energy states. The wavelengths used range from 1 μm to 100 μm . Raman spectra (predicted by Smekal in 1923) were first observed by C. V. Raman and K. S. Krishnan in 1928 (Raman & Krishnan, 1928) and C. V. Raman was rewarded the Nobel price in 1930 for the discovery of the effect. The energies depend on the vibrational force constants within the molecule and the spectrum provides information of the energies required for generating vibrations within a molecule. Raman spectroscopy uses both scattering and absorption, since the energy change caused by the specimen after being exposed to infrared energy is measured only on (inelastically) scattered light perpendicular to the incoming energy. The scattered light occurs at wavelengths that are shifted from the incoming light by the energies of molecular vibrations. For a vibration to be Raman active, there must be a change in the polarizability tensor. The polarizability depends on the molecular shape, and the Raman active components are the x^2 , y^2 , z^2 , xy , xz and yz coordinates. In order to extract information about force constants of bonding interactions within a molecule, from the energies of the vibrations, one must perform a series of measurements and compare similar compounds, such as corresponding deuterated species. In the thesis, Raman spectroscopy has merely been utilized as a fingerprint in order to compare different compounds. The frequencies of the most important (but often weak) Raman band originating from the metal-nitrogen symmetric stretching frequencies are in the range 200-400 cm^{-1} . The instrument used was an FT-Raman module FRA106/S in combination with an FT-IR spectrometer Bruker IFS66/S equipped with an FT-Raman accessory at IFM, Linköping University. Further reading about vibrational spectroscopy can be found elsewhere. (Nakamoto, 1997)

X-ray Diffraction in solid state (Crystallography)

The method is based on determination of the distances between interatomic planes within a crystal (Fig. 12). When energy in the form of X-ray radiation (0.7107 Å) hits a surface, in this case a plane in a crystal, the beam is scattered by the electrons. At a certain angle of the incident beam, the beams will be in-phase. (Fig. 12)

Then, the condition for diffraction is fulfilled according to Bragg's law;

$$n\lambda = 2d\sin\theta$$

where n = order of the diffraction pattern
 d = distance between atomic planes
 θ = angle of incident beam
 λ = wavelength of the radiation used

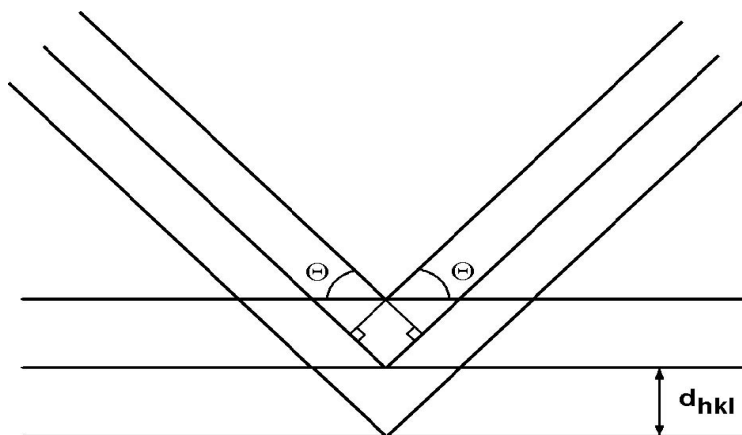


Fig. 12. A diffracted beam in a crystal

In 1912, Max von Laue showed that crystals are based on a three dimensional lattice, which scatters radiation with a wavelength in the vicinity of interatomic distances (X-rays). He received the Nobel Prize in physics in 1914. The method is widely used for structural determinations in solid state, and very exactly measures the average positions of high electron density in a crystal lattice. In the case when interactions with antiparallel orientation of a distorted metal ion coordination sphere lowers the energy (antiferrodistortive interactions), a weighted average bond distances will be detected, and thus differ from the distances present in the actual coordination geometry (Paper III). (Bersuker, 1996; Persson, Persson & Sandström *et al.*, 2002)

Two different approaches can be applied; single crystal diffraction and, when a single crystal is not possible to obtain, powder diffraction. The instrument used for single crystal diffraction was a Bruker SMART CCD 1 k diffractometer, (Bruker, 1995) and the instrument used for powder diffraction was a Stoe & Cie. (Stoe & Cie, GmbH) The crystal structures were solved by standard direct methods in the SHELXTL program package (Sheldrick, 1990) For a more thorough description of X-ray crystal diffraction, see for instance (Massa, 2000).

X-ray Diffraction in solution (LAXS)

Even if in solution, the structure of a complex cannot be regarded as totally random and in the short range a high degree of order is present. Contrary to the EXAFS technique, in the LAXS method all present atoms contribute to the oscillations. Furthermore, the damping of the intensity in EXAFS is less than in the LAXS method, (Persson, Sandström & Yokoyama *et al.*, 1995) resulting in possibilities of gaining different information from the same system, using the two methods. (Paper II and ref. therein) The structure information given by LAXS is in one dimension, the radial distribution function, displaying the interatomic distances. As it is extremely difficult to maintain the required temperature of a liquid ammonia solution during the long time (ca two weeks) for data sampling, the method had been used only on aqueous, dimethylsulfoxide and phosphorous donor solutions. The experimental set-up and theory of the data treatment and modelling have been presented elsewhere. (Sandström, 1978; Stålhandske, 1997)

Extended X-ray Absorption Fine Structure (EXAFS)

Structures in solution can favourably be investigated with EXAFS, which has been the main tool for determining the structures included in this thesis. When photoelectrons from the innermost K- and L-shells (core electrons) in an atom are excited, a photoelectron wave is produced. This outgoing wave can be scattered by the surrounding atoms (back-scatterers). The waves from the out-going and back-scattered photoelectron waves are subjected to destructive or constructive interference. This will result in minima and maxima, respectively, of the absorbed energy (Fig. 13), recorded before the electron returns back to the core hole.

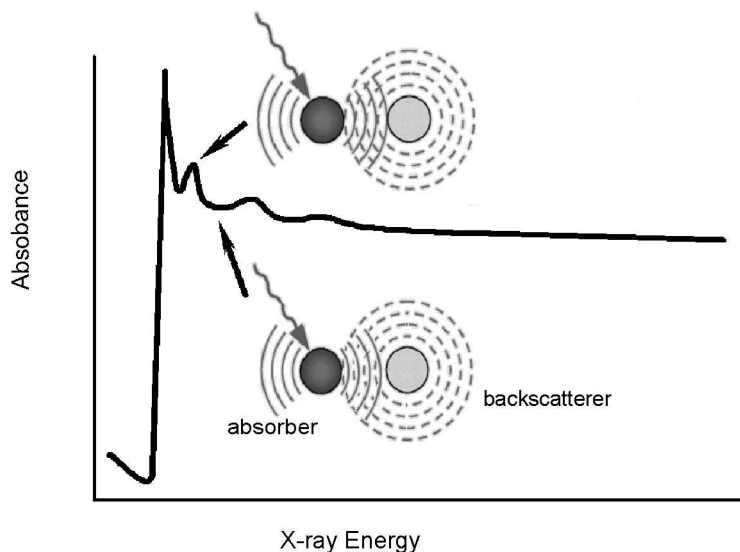


Fig. 13. An illustration of the scattered waves, interference pattern and the energy absorption resulting in EXAFS.

In principle, the information achieved from the sinusoidal curve is the density, the number of and distances to the back-scatterers surrounding the absorbing atom, as shown in Fig. 14. As this method determines the interatomic distances from the closest surroundings of an absorbing atom, it is complementary to the X-ray diffraction methods. The contributions to the EXAFS oscillations can be described in the EXAFS equation;

$$\chi_i(k) = \sum_j \frac{N_j \cdot S_o^2(k)}{k \cdot R_j^2} |f_{\text{eff}}(k)|_j \cdot \exp(-2k^2\sigma_j^2) \cdot \exp[-2R_j/\Lambda(k)] \cdot \sin[2kR_j + \phi_{ij}(k)]$$

in which

- N_j = Number of backscatterers in the j th shell
- R_j = Distance between the central atom i and the backscatterers in the j th shell in single backscattering (for multiple scattering, half of the total path length, $R_j = R_{\text{tot}}/2$)
- S_o^2 = Amplitude reduction factor due to multiple excitations, etc.
- f_{eff} = Effective amplitude function for each scattering path
- $\exp(-2k^2\sigma_j^2)$ = Debye-Waller factor in the harmonic approximation
- σ_j = Debye-Waller parameter accounting for thermal and configurational disorder
- $\exp[-2R_j/\Lambda(k)]$ = Mean free path factor
- $\Lambda(k)$ = Photoelectron mean free path
- ϕ_{ij} = Phase shift due to the coulomb potential of the central atom i and of the backscattering atom j

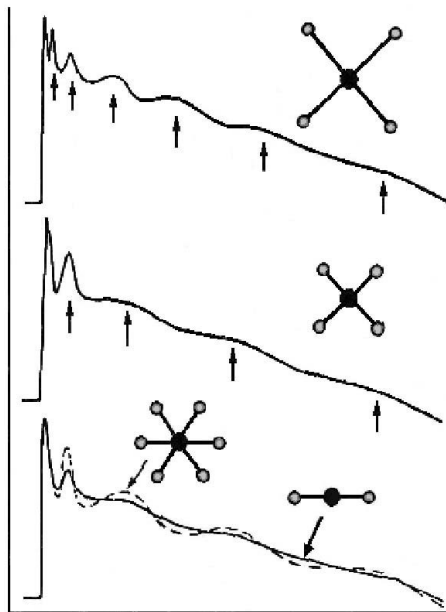


Fig. 14. A picture of the EXAFS extractable information. A short absorber back-scatterer distance results in low frequency oscillations, a long distance results in high frequency oscillations, and amplitude differences are caused by different numbers of nearest neighbours.

Data treatment includes energy calibration, background correction, normalization, "atomic background" removal and conversion from k -space via Fourier Transformation. The method has been described more thoroughly elsewhere. (Jahlilevand, 2000)

The amount of computer programs for evaluating EXAFS data is vast. Data included in the thesis has been treated with two different acknowledged programs EXAFSPAK, (George & Pickering, 1993) using the FEFF code (Zabinsky, Rehr & Ankudinov *et al.*, 1995) for calculations of k^3 -weighted model functions, using *ab initio* calculated phase and amplitude parameters, and the GNXAS program. (http://gnxas.unicam.it/XASLABwww/pag_gnxas.html, 15-Feb-2005) The reason for evaluating data with EXAFSPAK is the facile handling, which is fairly straightforward and if input data are correct, the result is considered reliable. The input to the GNXAS program is more advanced and includes potential and phase shift generation, signal calculation for reference geometries and advanced fitting of the experimental data. One of the advantages of using GNXAS for data treatment is the handling of the "atomic background" absorption, resulting from absorption when, in theory, no atoms are surrounding the absorbing atom. Another advantage is the treatment of double electron excitations in spectra, sometimes causing great problems with data treatment. In order to solve these problems, the GNXAS program was used for data treatment in parts of Paper II.

In an EXAFS measurement, a sufficiently high signal-to-noise ratio is needed and therefore a high X-ray flux is necessary. A synchrotron radiation source provides the energy flux, brilliance and also the high stability needed for an EXAFS experiment. All data have been collected at SSRL beamlines 4-1 at 3.0 GeV and a maximum current of 100 mA. A Si[220] double crystal monochromator was used.

Results and discussion

Copper(I), silver(I) and gold(I)

Ammonia solvation

The ammonia solvated copper(I) ions in liquid ammonia solution were analysed by EXAFS, and a mean Cu-N bond distance of 2.00 Å was obtained. This strongly indicates a trigonal configuration around copper(I), compared with previously analysed two-, three- and four-coordinated copper(I) complexes. (Paper I) A trigonal configuration is also supported by the formation of a third complex in aqueous ammonia, (Bjerrum, 1986b), lack of signals in the ^{63}Cu NMR spectrum, the pre-edge features that the trisamminecopper(I) ion exhibits at ca. 8984 eV in the EXAFS spectrum (Paper I) and the earlier assumption of a trigonal complex in the nitrate salt. (Zachwieja & Jacobs, 1989)

The geometry of the ammonia solvated silver(I) ion in solid trisamminesilver(I) perchlorate ($[\text{Ag}(\text{NH}_3)_3]\text{ClO}_4 \cdot 0.5\text{NH}_3$) was determined to be symmetrically trigonal with mean Ag-N bond distances of 2.263(6) Å and N-Ag-N bond angles

of 120° (Fig. 15 and Paper II). The AgN_3 entities are arranged in linear chains with a fairly short $\text{Ag}\cdots\text{Ag}$ distance ($3.278(2) \text{ \AA}$) in an almost identical way as previously found in the corresponding nitrate salt. (Zachwieja & Jacobs, 1989) The structure, determined by single crystal X-ray diffraction, was satisfactorily solved in space group P-31c (no 163). However, it cannot be ruled out that the symmetry of the space group results in a higher symmetry than the geometry of a specific silver(I) ion. (See method discussion on page 26). In the structure, the perchlorate anions are strongly disordered and partly occupied ammonia positions are present in the crystal lattice. This compound is thermally unstable, and even by grinding it before an EXAFS analysis, the trisamminesilver(I) perchlorate was deammoniated to linear bisamminesilver(I) perchlorate with a Ag-N bond distance of $2.126(8) \text{ \AA}$. The structure is similar to the one formed when bisamminesilver(I) perchlorate is crystallised from aqueous ammonia. (Nockemann & Meyer, 2002) A thermogravimetric analysis showed that when heating the compound to 673 K , further deammoniation occurred and less than one ammonia molecule was bound to silver(I) at this temperature.

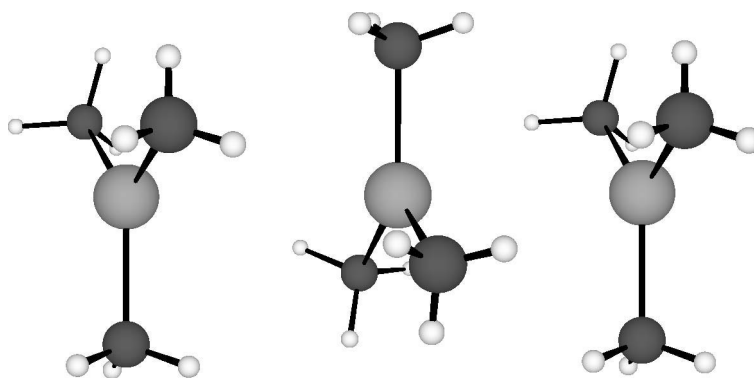


Fig. 15. Trisamminesilver(I) entities in the crystal lattice of $[\text{Ag}(\text{NH}_3)_3]\text{ClO}_4 \cdot 0.5\text{NH}_3$.

EXAFS data of liquid and aqueous ammonia solutions of silver(I) perchlorate (Paper II) reveal that the ammonia solvated silver(I) ion has different dominating solvate complexes in the two solvents. The mean Ag-N bond distance in liquid ammonia is much longer than in aqueous ammonia, $2.24(1)$ and $2.156(6) \text{ \AA}$, respectively, strongly indicating trigonal and linear configuration, respectively. The mean Ag-N bond distance of $2.24(1) \text{ \AA}$ in the trisamminesilver(I) complex in liquid ammonia is close to $2.263(6) \text{ \AA}$, found in solid $[\text{Ag}(\text{NH}_3)_3]\text{ClO}_4 \cdot 0.5\text{NH}_3$. In analogy with the hydrated silver(I) ion (Paper II), with highly irregular tetrahedral configuration and supported by the fairly large Debye-Waller parameter of trisamminesilver(I), it is possible that the trigonal $[\text{Ag}(\text{NH}_3)_3]^+$ complex in liquid ammonia has a lower symmetry than found in the crystallographic study. The Ag-N bond distance of $2.156(6) \text{ \AA}$ in the bisamminesilver(I) ion in aqueous ammonia solution is within the range of distances found in crystal structure determinations of linear bisamminesilver(I) complexes, (Maurer & Weiss, 1977; Zachwieja & Jacobs, 1989, 1992; Nockemann & Meyer, 2002) but shorter than a previous

determination of the Ag-N bond distance in the bisamminesilver(I) ion, by LAXS. (Maeda, Maegawa & Yamaguchi, *et al.*, 1979)

The structure of the ammonia solvated gold(I) ion in solid bisamminegold(I) tetrafluoroborate was not possible to determine by means of X-ray crystallography due to unstable crystals, but an EXAFS analysis provided structural data of the Au-N bond distances. The configuration of the ammonia solvated gold (I) ion in solid state, in liquid ammonia solution as well as in aqueous ammonia solution is linear with Au-N bond distances of 2.025(2), 2.026(3) and 2.022(2) Å, respectively. In solid state, no Au...Au distances could be detected according to the EXAFS analysis, as found in solid bisamminegold(I) bromide. (Mingos, Yau & Menzer *et al.*, 1995)

The dominating copper(I) and silver(I) species in aqueous ammonia are known to be linear, as previously determined by EXAFS and LAXS, respectively. (Maeda, Maegawa & Yamaguchi *et al.*, 1979; Lambie, Moen & Nicholson, 1994) As determined by Bjerrum, (Bjerrum, 1986a, b) both copper(I) and silver(I) ions form three-coordinated complexes, 27% and 5%, respectively, in 10 mol·dm⁻³ aqueous ammonia solution. This means that no changes in coordination number occur between metal ion solvation in aqueous and liquid ammonia solution, as the third ammonia ligand is coordinated because of an increased ammonia activity. Only the increased ammonia activity present in liquid ammonia is sufficient to obtain the highest available coordination number of the dominating species. The complex distribution curves of the copper(I) ion and the silver(I) ion in aqueous ammonia are displayed in Paper I, Fig. S1 and Paper II, Fig. 1.

Solvates of phosphites and phosphines

The solvation of the copper(I) ion in phosphorous donor solvents results in tetrahedral configuration in all investigated phosphite and phosphine solvents, both in solid state and solution. According to the EXAFS results, the Cu-P bond distances are 2.245-2.279 Å, in accordance with tetrahedral symmetry of the copper(I) ion. The copper(I) ion in phosphite and phosphine solutions was also analysed by ⁶³Cu NMR spectroscopy, the result showing nice, narrow peaks with ⁶³Cu-³¹P *J*-coupling resulting in quintets for the symmetric complexes in solution and in solid state. The complexes with bulky alkyl or π-electron donating aryl substituents were NMR silent because of an uneven distribution of the electrons, and thereby also of the ligands, around the copper(I) nucleus. The bulkiness of the substituent (measured as the "cone angle"; Paper I and Appendix B), causing steric restrictions from symmetric tetrahedral configuration, was well correlated to detected ⁶³Cu NMR signals. The recording of tetrakis(tri-isopropyl phosphite)copper(I), the complex detected possessing the largest detected ligand cone angle, 130°, was made possible by cooling the sample to 260 K. No detection was possible beyond a ligand cone angle of 130°, despite cooling. The bulkiness of triphenylphosphine causes severe steric restrictions in the coordination sphere of copper(I) complexes, and the mean Cu-P bond distance in three-coordinated triphenyl complexes in the database (Allen, Bellard, & Brice *et al.*, 1979) is as much as 2.29 Å.

The coordination chemistry of the even stronger electron acceptors silver(I) and gold(I) in the phosphorous donor solvents is more versatile. Silver(I) is tetrahedral in triethyl- and tri-*n*-butyl phosphite solution, with Ag-P bond distances of 2.470-2.476 Å, but probably three-coordinated in triphenyl phosphite and tri-*n*-butylphosphine solution with Ag-P bond distances of 2.421-2.452 Å. Plausibly, the phosphorous atoms in the latter solvents possess other electronic states than the alkyl phosphites, with abilities of vibronic mixing and thereby a lowering of the symmetry around the silver(I) ion (p. 18). Gold(I) is usually linear in strong electron donor solvents, such as liquid ammonia, due to the relativistic effects described in the next section. However, in both triethyl phosphite and tri-*n*-butylphosphine, the coordination figures are probably trigonal with Au-P bond distances of 2.353 and 2.345 Å, respectively. (Paper II)

Relativistic effects of gold

These determinations of the Au-L and Ag-L bond distances in linear configuration show that the silver(I) and gold(I) complexes formed in the investigated solvents are anomalous in the sense that the larger gold(I) ion (1.51 Å; octahedral) (Shannon, 1976) forms shorter M-L bonds than the silver(I) ion (1.29 Å; octahedral). The short Au-L bond distances exist owing to the relativistic effects of gold(I).

Relativistic effects can qualitatively be attributed to the high speed of all electrons if they move near a heavy nucleus (quantitatively seen in Fig. 16). The consequent mass increase will lead to an energetic stabilisation and radical contraction. For the *s*- and *p*-orbitals, this will be the main effect. The contraction of those orbitals leads to a stronger screening of the nuclear attraction and hence to a destabilisation and expansion on the *p* and *f* orbitals (*indirect relativistic effects*). The third most important relativistic effect is the *spin-orbit coupling*, which also increases roughly like Z^2 and becomes especially important. Of the group 11 metals, only silver acts “normally”. Gold is relativistic and copper has a very compact *d* shell with strong electron-electron repulsion, which may be related to the existence of copper(II). (Pyykkö, 2004)

One of the manifestations of the relativistic effects is a bond-length contraction, which also correlates roughly with Z^2 (Fig. 16). The Au-L bond distances can be

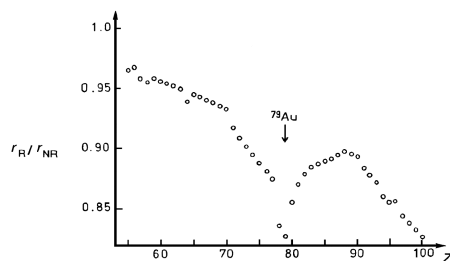


Fig. 16. The ratio of relativistic/non-relativistic 6s shell radii in the atomic ground states of the elements 55-100.

Table 3. *M-L bond distances ($r/\text{\AA}$) in copper(I), silver(I) and gold(I) complexes in solution, formed in decreasingly strong electron donor solvents. ^a(Hertzberg, 1950), ^b(Kickelbick & Schubert, 1997), ^c(Bachman & Andretta, 1998), ^dPaper II, in solution, ^e(Allen, Ballard & Brice et al., 1979), ^f(Lamble, Moen & Nicholson, 1994)*

Metal ion	H ⁻ ^a	PH ₃ ^b	(PR ₃) ₂ ^c	(PR ₃) ₃ ^d	(PR ₃) ₄ ^e	(NH ₃) ₂ ^d	(P(OPh) ₃) ₃ ^d
Copper(I)	1.463	2.252	2.197 ^e	2.295 ^e	2.269	1.88 ^f	-
Silver(I)	1.617	2.413	2.420	2.452	2.658	2.16	2.42
Gold(I)	1.524	2.266	2.315	2.345	2.634	2.03	2.35
r(Ag-L) – r(Au-L)/ \AA	0.093	0.147	0.105	0.107	0.024	0.13	0.07

similar or shorter than the corresponding Ag-L bonds, and simultaneously make the Au-L bonds stronger than those of the corresponding Ag-L bonds. (Schwerdtfeger, 2002; Pyykkö, 2004)

There is no obvious trend in the effects on the M-L bond shortening between silver(I) and gold(I) and solvent donor strength. The gold(I) ions with tetrahedral configuration are less affected than the ones in linear or trigonal configuration.

Copper(II)

The ammonia solvated copper(II) ion has an axially elongated octahedral configuration, in solid state, as well as in solution (Paper III) due to the JTE (p. 18). The four Cu-N_{eq} bond distances are 2.021(5) and 2.023(5) \AA , and the two Cu-N_{ax} bond distances are 2.76(2) and 2.78(2) \AA in liquid and aqueous ammonia solution, respectively, according to EXAFS results. In solid state, using single crystal X-ray diffraction, the ammonia solvated hexaamminecopper(II) ion in [Cu(NH₃)₆](ClO₄)₂ was determined to have symmetric octahedral configuration with a mean Cu-N bond distance of 2.091(13) \AA (cubic space group Fm3m). However, according to the EXAFS results, the orientation of the longer axial Cu-N bond in the ammonia solvated copper(II) ion must be randomly orientated in the crystal lattice (Fig. 17 and p. 26), as Cu-N_{eq} and Cu-N_{ax} bond distances of 1.996(3) and 2.70(2) \AA , respectively, were obtained. A Differential Scanning Calorimetry (DSC) analysis of the hexaamminecopper(II) perchlorate crystals was performed, and the result showed that a temperature-dependent phase transition reversibly takes place at 147 K, probably the result of a re-orientation of the Jahn-Teller distorted hexaamminecopper(II) complexes with a new alignment in the same direction for all of the complexes, and consequently a lower symmetry of the crystal structure of the compound.

The difference between the equatorial and axial bond distances is similar to the ones determined by X-ray crystallography in the hexaamminecopper(II) chloride salt, but larger than and the difference in the bromide salt. (Distler & Vaughan, 1967) Compared with two other hexaamminecopper(I) complexes, (ICSD, 2004) the bond distances are similar (Paper III; Table 1)

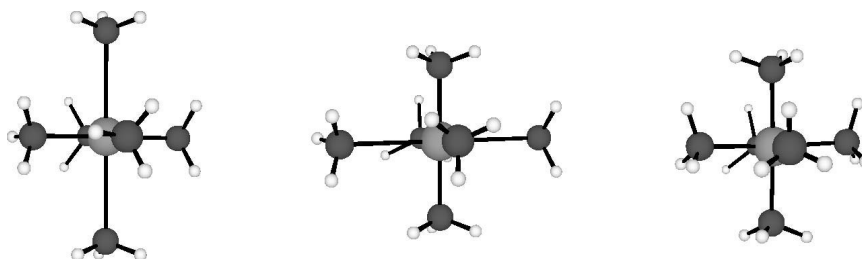


Fig. 17. Possible orientations of the JT-distorted hexaamminecopper(II) entities in the crystal lattice of $[\text{Cu}(\text{NH}_3)_6](\text{ClO}_4)_2$ at 295 K.

In liquid ammonia solution, the EXAFS results show a slightly longer equatorial bond distance, 2.021(5) Å, and the about same one, 2.76(2) Å, as in solid state. The liquid ammonia solvated copper(II) ion has been investigated before, using the information in the XANES spectrum, combined with computational methods. (Valli, Matsuo & Wakita *et al.*, 1996) The result of that study was a most probable copper(II) geometry of pentagonal pyramidal, with the copper(II) ion closer to the bottom, lifted above the equatorial nitrogen plane. The computational method has been questioned before, (Pranowo & Rode, 1999) and this model could not be applied on our EXAFS data.

Theoretical calculations of copper(II) in liquid ammonia suggested that a 4+2 configuration (four long equatorial and two short axial bonds) in the JT distorted structure was a probable solution to the problem of determining the structure. (Schwenk & Rode, 2004) However, the experimental mean value of 2.10 Å in the crystal structure determination of the solid compound, combined with the dominating short Cu-N bond distance of 2.026 Å in the EXAFS determination do not suggest that an axially compressed structure is the correct one.

In concentrated aqueous ammonia solution, the dominating species are the tetra- and pentaamminecopper(II) complexes, as the sixth complex in aqueous ammonia solution is very weak (Paper III, Fig. S1). However, as in the case of the copper(I) and silver(I) ions in the aqueous ammonia system, the coordination number of the copper(II) ion is substantially a matter of ammonia activity. By EXAFS, it is not possible to determine if the ligand atoms are nitrogen or oxygen. The equatorial and axial bond distances are very similar to the ones in the hexaamminecopper(II) complex in solid state; 1.996(3) and 2.70(2) Å, respectively. This result is also consistent with the crystallographically determined copper(II) coordination in $[\text{Cu}(\text{NH}_3)_4][\text{CuCl}_2]$. (Baglio & Vaughan, 1970)

The copper(II) ion is six-coordinated in aqueous solution (Ohtaki & Radnai, 1993) as well as in the solid hydrates. (Persson, Persson & Sandström *et al.*, 2002) According to quantum mechanical/molecular mechanical molecular dynamics simulations, both five- and six-coordination are equally energetically favourable, both in aqueous and ammonia solutions. (Schwenk & Rode, 2004)

Zinc(II), cadmium(II) and mercury(II)

The ammonia solvated "intermediate" zinc(II) and cadmium(II) ions are symmetrically tetrahedral and octahedral, respectively in solid state and liquid ammonia solution (Paper III). (Gans & Gill, 1976; Hillebrecht, Thiele & Koppenhoefer *et al.*, 1994) EXAFS results give mean Zn-N bond distances of 2.020(3), 2.03(1) and 2.016(6) Å in solid state, liquid ammonia and aqueous ammonia solution, respectively. This result is in accordance with solid state structures of the tetraamminezinc(II) ion (Paper III, Table 2) with a mean Zn-N bond distance of 2.032 Å. The mean Cd-N bond distances are determined to 2.34(2), 2.35(1) and 2.35(1) Å in solid state, liquid ammonia and aqueous ammonia solution, respectively. The crystal structure of solid Cd(NH₃)₆Cl₂ was solved in space group Fm3m (No 225) and shows a mean Cd-N bond distance of 2.341(4) Å in a symmetric octahedral environment.

The configuration of the ammonia solvated mercury(II) ion in solid state is distorted tetrahedral and subject to PJTE, or both JTE and PJTE (pp. 17-18), as the results from single crystal X-ray diffraction of [Hg(NH₃)₄](ClO₄)₂ shows (Paper IV and Fig. 18). The crystal structure has been determined at room temperature (Paper IV) and at 170 K, (Nockemann & Meyer, 2003) resulting in different space groups, orthorhombic Pmna (No. 62) and monoclinic P2₁/c (No. 14), respectively. A DSC analysis shows that the crystals undergo phase transitions at ca. 230 and 270 K, of which the transition at 230 K is reversible. The result is a lowered symmetry of the space group at lowered temperature, as a JT- and/or PJT type instability can trigger a temperature dependent symmetry breaking in a crystalline phase (p. 18). The structure determinations of two of the phases of tetraammine-mercury(II) perchlorate (at 295 K and 170 K) show two shorter and two equidistant, longer Hg-N bond distances (C_s symmetry; Fig. 18) and two equidistant, shorter and two equidistant, longer Hg-N bond distances (C_{2v} symmetry; Table 2), respectively.

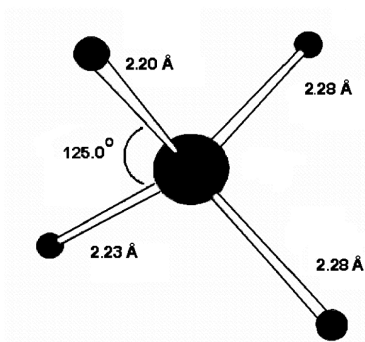


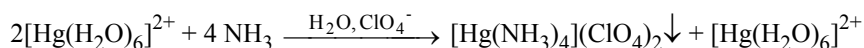
Fig. 18. The tetraammine-mercury(II) entity at 295 K.

Solid tetraamminemercury(II) perchlorate is thermally unstable and a thermogravimetric analysis showed a deammoniation of tetraamminemercury(II) perchlorate at 400 K, when linear bisamminemercury(II) perchlorate is formed. (Paper IV, Fig. 1) Even at room temperature, 6-7% of the tetraamminemercury(II) perchlorate was deammoniated as a result of grinding prior to the EXAFS analysis. The instability of the tetraamminemercury(II) perchlorate is displayed as an extra peak in the Fourier Transform of the EXAFS spectrum, emanating from the Hg...Hg contribution in the linear bisamminemercury(II) perchlorate at 3.41 Å (Paper IV).

From EXAFS combined with powder diffraction results, the structure of bisamminemercury(II) perchlorate has been deduced to consist of a mercury(II) network structure with Hg...Hg distances of 3.41 Å and with a linear ammonia coordination around each mercury(II) ion with a bond distance of 2.064(3) Å. The mercury(II) ions are probably connected through perchlorate oxygens found at a bond distance of 2.83 Å, according to the EXAFS results. The chloride ions are likely to be situated in the middle of the network cavities at a distance of 4.05 Å from the mercury(II) ions, determined by EXAFS as well as by powder diffraction. As the preference of linear configuration around mercury(II), due to the closeness in energies of the 6s and 5d orbitals is well known, the stability of a bisamminemercury(II) complex is not surprising.

In both liquid and aqueous ammonia solution, the same tetrahedral ammonia solvated mercury(II) ion is observed, supported by the mean Hg-N bond distances of 2.24(2) and 2.229(3) Å, respectively. The mercury(II) complex formation in aqueous ammonia slightly differs from the copper(I) and silver(I) ions, discussed on p. 31, for which only a minor amount of the trigonal complexes are formed in concentrated aqueous ammonia solution. The complex distribution function of the mercury(II) ion in aqueous ammonia is displayed in Paper IV, Fig. S1. The mercury(II) tetrahedra are presumably distorted in solution in a similar way as in the solid state, as the Debye-Waller parameters in the EXAFS analyses, which displays the amount of thermal and configurational disorder, are fairly high and equal to the one in solid state (Paper IV).

¹⁹⁹Hg NMR studies of aqueous ammonia solvation of the mercury(II) ion in a system with net molar ratios NH₃/Hg²⁺ of 0-130 show a broad distribution of shifts within a range of 1200 ppm. At low ratios, an almost quantitative precipitation of tetraamminemercury(II) perchlorate occurs, leaving six-coordinated hydrated mercury(II) ions in the aqueous phase. At higher ratios the shift approaches 1200 ppm, the shift of the tetraamminemercury(II) ion in solution. A single resonance is exhibited because of the very fast ligand exchange on the NMR time scale. The reaction occurring at low net molar ratio could be described as:



The ¹⁹⁹Hg chemical shift shows a pronounced dependence on the coordination number of the mercury(II) ion in different solvents, resulting in over 1200 ppm difference between the distorted tetrahedral solvates of *N,N*-

dimethylthioformamide and ammonia and the octahedral solvates of water and dimethylsulfoxide. Therefore ^{199}Hg NMR investigations can be used as a probe of the basic configuration of the mercury(II) ion. An attempt was also made to correlate the spin-lattice relaxation times of the ^{199}Hg nucleus in the solvates with its coordination geometry. (Maliarik & Persson) The correlation could be made according to the restrictions discussed on page 20. The T_1 value of the $[\text{Hg}(\text{NH}_3)_4]^{2+}$ species is close to the value of the $[\text{Hg}(\text{SCNH}(\text{CH}_3)_2)_4]^{2+}$ solvate complex, 3.00 and 2.61 s, respectively, while the relaxation times of the pseudo-octahedral species, $[\text{Hg}(\text{OH}_2)_6]^{2+}$ and $[\text{Hg}(\text{OS}(\text{CH}_3)_2)_6]^{2+}$, are longer, ca. 7 s. (Paper IV)

Mercury(II) halides

The mercury(II) chloride and bromide compounds are completely dissociated in liquid ammonia solution and mercury(II) is present as tetraamminemercury(II) ions (Paper V). Both the Hg-N bond distances of 2.251(8) and 2.21(2) Å, respectively, and the Debye-Waller parameters from the EXAFS results are similar to the tetraamminemercury(II) ion in liquid ammonia. However, in solid state, Raman spectroscopic measurements and powder diffraction data suggest that the dominating species is a bisamminemercury(II) complex. The dimensions of the unit cells of the solid phases were analyzed by powder diffraction, showing that they most probably have the same structures as presented in 1936, bisamminemercury(II) chloride and bisamminemercury(II) bromide. (MacGillavry & Bijvoet, 1936) In trialkyl phosphite and trialkylphosphine, the permittivity is too low to keep the charged solvated mercury(II) ions in solution, and instead ion-pairs are formed in solid state, and the compounds shall be regarded as salts of solvated metal ions.

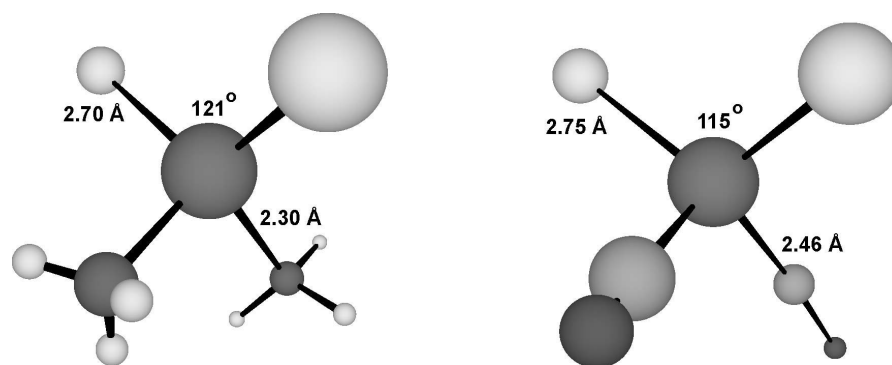


Fig. 19. The pseudo-tetrahedral probable $\text{Hg}(\text{NH}_3)_2\text{I}_2$ (left) and structurally determined $\text{Hg}[\text{P}(\text{OC}_4\text{H}_9)_3]_2\text{I}_2$ (right) solvate structures (alkyl chains omitted for clarity).

The mercury(II) iodide is not dissociated in liquid ammonia solution, and the two iodide ions remain bonded to mercury(II) in the inner coordination sphere, giving a pseudo-tetrahedral complex, assumably similar to the one in $[\text{HgI}_2(\text{NH}_3)_2]\text{S}_4\text{N}_4$, (Martan & Weiss, 1984) shown in Fig. 19, with the Hg-I and Hg-N bond distances and angles displayed. The structure can also be compared with the tri-*n*-butyl phosphite solvated mercury(II) iodide, with similar bond

distances and angles. (Fig. 19 and Paper V) However, in the strongest electron-pair donor surveyed, tri-*n*-butylphosphine ($D_S=76$), mercury(II) iodide is completely dissociated, and in this extreme case a linear structure around the mercury(II) ion with Hg-P bond distances of 2.468(4) Å is formed in a melt with the mercury(II):iodide:phosphines ratios 1:2.0:3.0, as determined by LAXS (Paper V).

When solid mercury(II) chloride was dissolved in liquid ammonia, a surprising phenomenon appeared. A three-phase system emerged, consisting of a new solid phase, $\text{Hg}(\text{NH}_3)_2\text{Cl}_2$ (s), and two immiscible liquid phases. The liquid phases have been analysed by several methods and the lower, dense phase contains a high concentration of tetrahedral mercury(II) ions, most probably present as $\text{Hg}(\text{NH}_3)_4^{2+}$ entities, hydrogen bonded to chloride ions in a network. The light phase contains a fairly low concentration of $\text{Hg}(\text{NH}_3)_4^{2+}$ complexes and chloride ions in liquid ammonia solution, as determined by EXAFS and Raman spectroscopy.

The Raman spectrum of the dense phase suggests that there is still a large amount of ammonia present in this solution, but the $2\delta_1$ band from the overtone of the N-H bending mode resembles the broader one in aqueous ammonia, much more than the strong and sharp band in liquid ammonia. The ^{199}Hg NMR spin-lattice relaxation (T_1) of the mercury(II) ions was only possible to determine in the dense phase. The result was a longer value of T_1 than in the tetrahedral complexes, 5.28 s, (Paper V; Table 5) presumably an effect of hydrogen bonding to the chloride ions. The volumetric proportions of the solid phase and upper and lower liquid phases depend on the amount of HgCl_2 (s) added to the liquid ammonia solution. A larger amount of HgCl_2 (s) added results in a relative larger volume of the dense liquid phase. These kinds of liquid-liquid phase separations in liquid ammonia have been observed before (p. 14), but so far only produced from alkali metals, oxidized in the solution, and where the dense phase is the low metal concentration phase. No originally oxidized metals have previously been reported to give liquid-liquid phase separations in liquid ammonia.

The complex formation of $[\text{HgI}_n]^{(2-n)+}$ species in liquid ammonia solution was investigated using ^{199}Hg NMR spectroscopy. Again, a very large range in shift is seen, as the shift of the mercury(II) ion ranges from 1200 ppm in the PJT distorted tetraamminemercury(II) complex in liquid ammonia to -1700 ppm in the tetraiodomercurate(II) complex in liquid ammonia. Strong electron-pair donor ability and large size of the ligand promote large shielding of the ^{199}Hg nucleus. The species formed with the highest available coordination number is four, in the tetraiodomercurate(II) ion. The samples containing the highest iodide concentrations were also analyzed by EXAFS and Raman spectroscopy, and the mean Hg-I bond distance in the $[\text{HgI}_4]^{2-}$ complex is 2.77 Å, which strongly indicates a tetrahedral configuration, compared with bond distances in solid state. (ICSD, 2004)

The electron-pair donor abilities are reflected in the solvation of the mercury halides; the X-Hg-X angle decreases with increasing donor strength of the solvent. In liquid ammonia, a fully ammonia solvated tetraamminemercury(II) ion from the chloride and bromide compounds displays the strong electron donor properties of

this solvent. Also the Hg-X bond distance and symmetric stretching frequencies are dependent on the solvent donor strength, a fact used in the construction of the D_S scale (p. 17; Sandström, Persson & Persson, 1990) In the case of tri-*n*-butyl phosphite, the I-Hg-I angle is 115° and in the liquid ammonia solvated mercury(II) iodide the angle is probably similar. The tri-*n*-butylphosphine solvated mercury(II) ion formed from the iodide compound certainly reflects a very strong solvation in this solvent. The Hg-X bond distance (Å) could be correlated to some extent to the Hg-X symmetric stretching wave number (cm^{-1}), (Stålhandske, 1996) and the two mercury (II) iodide solvate structures analysed are fairly well within the linear correlation range described before.

In the Raman measurement of mercury(II) iodide in liquid ammonia, the band from the Hg-I symmetric stretching frequency differed by 11 cm^{-1} from the result reported before. (Gardiner, Haji & Straughan, 1978) Our investigated solution was much more dilute ($\text{Hg}:\text{NH}_3$; 1:66) compared with the previously reported one (1:7), and it is likely that in the latter, more concentrated solution, some kind of association between the mercury(II) species did take place. As the previously reported electron-pair donor ability, expressed as the D_S number, of liquid ammonia is based on results from the Hg-I symmetric stretching wave number of the concentrated solution, (Sandström, Persson, & Persson, 1990) a revision from $D_S = 69$ to $D_S = 56$ is appropriate.

Indium(III) and thallium(III)

As the indium(III) ion is regarded as a "hard" electron-pair acceptor, the influence from covalent attraction is not assumed to be of great importance. Thallium(III), on the other hand, regarded as "soft", isoelectronic with the gold(I) and mercury(II) ions, might display a distortion from a regular symmetry. However, both indium(III) and thallium(III), do adopt octahedral conformation in liquid ammonia solution, with In-N and Tl-N bond distances of 2.232(7) and 2.29(2) Å, respectively. (Paper VI). Even though the thallium(III) ion is soft, the octahedral configuration is maintained, presumably because of the high charge of the ion. On the other hand, the Debye-Waller parameter in the EXAFS results is relatively large and the T_1 relaxation time of the ammonia solvated thallium(III) ion is significantly shorter than in the octahedral hydrated and dimethylsulfoxide solvated ones, as determined by ^{205}Tl NMR. (Paper VI) This may imply that the thallium(III) ion, parallel to the mercury(II) ion in aqueous solution (Mink, Németh & Hajba *et al.*, 2003) is subject to PJTE, and has a slightly distorted octahedral geometry.

When comparing the difference in M-N and M-O bond distances of the Group 13 trivalent metal ions, (Paper VI) a trend is obvious; the differences are larger for smaller and "hard" ions, and smaller for the larger and more "soft" metal ions. The "hard" ions are less prone to be solvated in the strong electron-pair donor solvent liquid ammonia than in water.

Metal ion solvation in liquid ammonia and aqueous solutions

In order to see any trends in difference between metal ion solvation in liquid ammonia and aqueous solution, Table 5 was constructed for comparison of the metal ion coordination figures.

When three of the “soft” metal ions are transferred from aqueous solution to liquid ammonia solution, a change of the coordination geometry occurs; tetrahedral to trigonal for copper(I), distorted tetrahedral to trigonal for silver(I), and distorted octahedral to distorted tetrahedral for mercury(II). This also occurs in the case of the “intermediate” zinc(II) ion (octahedral to tetrahedral) A lowering of the symmetry around a metal ion is most likely to occur for strong electron-pair acceptors in strong electron-pair donor solvents, when a significant degree of covalent bonding is involved. (pp. 17-18) A coordination change also takes place for the “intermediate” zinc(II) ion, but not for the “intermediate” cadmium(II) ion. Since vibronic coupling is only possible when the orbitals are sufficiently close in energy, the reason is probably that the electronic states of the zinc ion are close enough to mix, and thereby it is also subject to PJTE. Thus, a coordination change cannot be ruled out for a borderline/hard metal ion.

The hydrated silver(I) ion is the only surveyed metal ion with a coordination change between solid phase and solution; linear in the only isolated structurally determined silver hydrate, (Makhmudova, Sharipov & Khodashova *et al.*, 1985) while in solution it adopts highly irregular tetrahedral configuration. The ammoniated zinc(II) ion has been structurally determined as both tetrahedral and octahedral in solid state.

As even the very softest metal ions do not change their coordination number when they are transferred from concentrated aqueous ammonia solution to liquid ammonia, one can assume that for the weak electron-pair acceptors, the configuration is the same in aqueous ammonia as in liquid ammonia.

Table 4. *The number of ligands surrounding solvated d^{10} metal ions in liquid ammonia and liquid water. (Johansson, 1992; Ohtaki & Radnai, 1993; Persson, Penner-Hahn & Hodgson, 1993; Mink, Németh & Hajba *et al.*, 2003; This work)*

	NH ₃ /H ₂ O		NH ₃ /H ₂ O		NH ₃ /H ₂ O			
Cu(I)	3	4	Zn(II)	4	6	In(III)	6	6
Ag(I)	3	2+2	Cd(II)	6	6	Tl(III)	6	6
Au(I)	2	*	Hg(II)	4	6			

* Oxidizes to Au(III) in aqueous solution.

d^{10} Metal ion solvation in strong electron-pair donor solvents

Knowledge of the electron pair donor properties of a solvent, based on the D_S scale, cannot straightforwardly predict the configuration around a specific metal ion, regarding a lowering of symmetry within complexes formed with a large degree of covalent bonding (Table 5). The symmetry also depends on the properties of the donating atom. The copper(I) ion is tetrahedral in DMTF (slightly distorted) and trigonal in liquid ammonia but in the very soft solvent tri-*n*-butylphosphine ($D_S=76$) with a phosphorous donor atom, the configuration is tetrahedral.

The coordination number in the soft solvent solutions is sometimes lowered in solid state, as for the solid *N,N*-dimethylthioformamide solvated silver(I) (forming a dimer). (Table 5). Even if the coordination number is kept, the solid solvates might be thermally unstable, as in the case of trisamminesilver(I) perchlorate and tetraamminemercury(II) perchlorate (pp. 30 and 36). The trisamminesilver(I) compound is very unstable, with ammonia losses beginning at ca 440 K, and less than one ammonia bound per silver(I) ion is left at ca 670 K. The tetraamminemercury(II) compound is thermally more stable in a linear configuration, beginning to form at ca 400 K.

Changes in coordination numbers are present in the solvates produced with metal ions possessing low charge. The gold(I) ion, and also the mercury(II) ion, are also subject to relativistic effects (p. 32), with 6s orbital contraction taking over the occasional PJTE, as the energy gap between the different electronic states will be too large for the PJTE to be effective. The zinc(II) ion is tetrahedral also in *N,N*-dimethylthioformamide, a fact that must be ascribed to PJTE, as no steric repulsion of the ammonia or *N,N*-dimethylthioformamide ligands is present. (Stålhandske, Persson & Sandström *et al.*, 1997)

Table 5. The number of ligands surrounding d^{10} metal ions in soft solvents, in solution/solid state. ; Stålhandske, Persson & Sandström *et al.*, 1997 (Allen, Bellard & Brice *et al.*, 1979; Stålhandske, Stålhandske & Persson *et al.*, 2001; This work)

	DMTF/	NH ₃ /POR ₃ /		PR ₃		DMTF/	NH ₃
Cu(I)	4	3/3	4	4	Zn(II)	4/4	4/4
Ag(I)	4/3	3/3	3/3-4	3	Cd(II)	6/6	6/6
Au(I)	2/2	2/2	3	3/2-4	Hg(II)	4/-	4/4

Highlights

The most important findings in this thesis are the trigonal coordination of the copper(I) and silver(I) ions in liquid ammonia. The earlier supposed change of coordination number between the ammonia solvated silver(I) ion in aqueous ammonia and liquid ammonia solution can thus be ruled out, as the ammonia coordination is a matter of ammonia activity.

A JT-distorted octahedral configuration of copper(II) in liquid ammonia has been established, as EXAFS data are consistent with the solid state structure and previously crystallographically determined structures.

Not being part of the liquid ammonia and phosphorous donor solvent investigation, but included in Paper II, the very distorted tetrahedral configuration of the hydrated silver(I) ion was reported. The coordination geometry has been a question mark for quite some time. (Maeda, Maegawa & Yamaguchi *et al.*, 1979; Yamaguchi, Johansson & Holmberg *et al.*, 1984; Seward, Henderson & Charnock *et al.*, 1996; Moreno, 1998) The suggested model with two shorter and two longer silver-oxygen bonds, fitting both LAXS and EXAFS data seems to be the most probable one presented so far.

Many metal-ammonia liquid-liquid phase separated systems of alkali metals dissolved in liquid ammonia producing solvated electrons have been presented, the latest one containing rubidium. Here, the first discovered liquid-liquid phase separated metal ion solution (mercury(II) chloride) is presented, even though this solution does not produce solvated electrons. In contrast to the metal-liquid ammonia solutions, the dense phase in the mercury(II) chloride-ammonia system is also the one with the higher metal concentration.

The electron-pair donor strength of liquid ammonia has been revised to a lower D_S number of 56.

Future aspects

The mechanisms behind the configurations formed in strong electron-pair donor solvents together with strong electron acceptor metals are most interesting. As the configurations are different with different donor atoms although the electron-pair donor abilities are similar, the available orbitals taking part in bonding and their possibilities of mixing, including vibronic coupling and force constants must be decisive. These properties are in the scope of theoretical physical chemistry and could most probably be treated using (Pseudo) Jahn-Teller Effect theory. Especially the physical reasons for the 2+2 and trigonal (distorted?) configurations of the hydrated and ammonia solvated silver(I) ions, respectively, would be of interest to investigate further.

A challenging task would be to construct a new scale for the estimation of electron-pair acceptor abilities of “soft” metal ions, using the information from their coordination properties of complexes in different strong electron-pair donor solvents.

Structures of metal complexes are important in biological systems; approximately one third of all proteins and enzymes purified to apparent homogeneity have been estimated to require metal ions as cofactors for biological functions. (Holm, Kennepohl & Solomon, 1996) Revealing the preferred nitrogen coordination geometries of metal ions in different proteins, important to the biological functions of *e.g.* enzymes, is facilitated when the non-aqueous solvate structures are known.

The question of possibilities of life in liquid ammonia was raised in a Swedish popular scientific magazine, (Wallinder, 2004) in an article dealing with extraterrestrial life. The structures of liquid water and liquid ammonia are similar, but as stated on page 11, the potential of electron transport in liquid ammonia is much smaller. Therefore, is electron transport a requirement for any kind of biological process? Could life exist in liquid ammonia?

Acknowledgements

First of all, I would like to thank my supervisor, Ingmar Persson, for sharing parts of vast chemistry knowledge and guiding me through this process. All obstacles towards reliable results that turn up have been handled with enthusiasm, either by solving them immediately or letting them mature, and then solve them. Occasionally the key turned out to be another choice of route.

My enthusiastic co-supervisor Misha Maliarik has also contributed a lot in suggesting methods I had never thought of before (and performing them), although I believe your enthusiasm has declined as I try to make you work. My other co-supervisors, Vadim Kessler and Magnus Sandström have also contributed to results, pictures and fruitful discussions.

Other persons who have assisted me (a lot when there was time) are Lasse Eriksson and Alirheza Abassi at Stockholm University. My mentor during a year, Åke Danielsson (former Amersham Biosciences), should also be mentioned for exchanging thoughts about science, career and life.

I am very grateful to the persons who helped me getting started; Ann-Sofi, Lena, Camelia, Christina and Farideh (then at KTH). Corine and Rolf assisted me with NMR measurements and Bernt has always been providing materials when the students are around for lab work. Daniel and Christian have both been supporting me a lot in all computer-related issues! I thank ALL former and present colleagues for nice talks in the “fika-room”, especially Cissi, for being such an interested/ing chemistry- and life-discussing roommate.

Utan er; Min Familj, Mille, Erik och Axel, skulle livet ha varit både tråkigare och svårare, det är ju ni som är det viktigaste i mitt liv! (Miss Polly har också bidragit till avkoppling). Jag är otroligt tacksam för all hjälp med barnpassning och för allt stöd jag fått från er, mamma Berit och svärmor Ingegerd.

JLT and NL Faculties are acknowledged for giving me a Ph. D. position, and the Swedish Research Council for financial support of materials and travelling during this time. Portions of this research were carried out at the Stanford Synchrotron Radiation Laboratory, a national user facility operated by Stanford University on behalf of the U.S. Department of Energy, Office of Basic Energy Sciences. The SSRL Structural Molecular Biology Program is supported by the Department of Energy, Office of Biological and Environmental Research, and by the National Institutes of Health, National Center for Research Resources, Biomedical Technology Program.

References

- AAA Ammonia-Resource and Reference Center, NH₃ org. resource base.
<http://nh3.org/refer/nh3ref1.html#physical%20properties%20chart>;
pp. 1-5 (accessed 2-Jan-2005)
- Agmon, N. 1995. The Grotthuss mechanism, *Chemical Physics Letters* 244, 456.
- Ahrland, S., Chatt, J. & Davies, N.R. 1958. The relative affinities of ligand atoms for acceptor molecules and ions, *Quarterly Reviews* 12 (London), 265-276.
- Alfa Aesar laboratory chemical suppliers and distributors. <http://www.alfa.com> (accessed 2-Jan-2005)
- Alkali Metals. http://www.alkalimetals.com/specs/tri_phenyl_phosphine_specs.html
(accessed 9-Dec-2004)
- Allen, F.H., Bellard, S., Brice, M.D., Cartwright, B.A., Doubleday, A., Higgs, H., Hummelink, T., Hummelink-Peters, C.G., Kennard, O., Motherwell, W.D.S., Rodgers, J.R. & Watson, D.G. 1979. The Cambridge Crystallographic Data Centre: computer-based search, retrieval, analysis and display of information., *Acta Crystallographica Section B* 35, 2331.
- Bachman, R.E. & Andretta, D.F. 1998. Metal-ligand bonding in coinage metal-phosphine complexes: The synthesis and structure of some low-coordinate silver(I)-phosphine complexes, *Inorganic Chemistry* 37, 5657-5663, and references therein.
- Baglio, J.A. & Vaughan, P.A. 1970. The structures of the tetraamminecopper(II)dihalocuprates(I) II. The structures of Cu(NH₃)₄(CuBr₂)₂ and Cu(NH₃)₄(CuCl₂)₂·H₂O, *Journal of Inorganic and Nuclear Chemistry* 32, 803-810.
- Bausenwein, T., Bertagnolli, H., David, A., Goller, K., Zweier, H., Töheide, K. & Chieux, P. 1994. Structure and intermolecular interactions in fluid ammonia: An investigation by neutron diffraction at high pressure, statistical-mechanical calculations and computer simulations, *Journal of Chemical Physics* 101, 672-682.
- Bersuker, I.B. 1996. *Electronic structure and properties of transition metal compounds. Introduction to the theory*. John Wiley & Sons, Inc., 605 Third Avenue, New York, NY.
- Bersuker, I.B. 2001. Modern aspects of the Jahn-Teller effect theory and applications to molecular problems, *Chemical Reviews* 101, 1067-1114.
- Bjerrum, J. 1986a. Metal amine formation in solution. XXV. The stability constant of the triammine copper(I) complex, *Acta Chemica Scandinavica, Series A: Physical and Inorganic Chemistry*. A40, 233-235.
- Bjerrum, J. 1986b. Metal amine formation in solution. XXVI. Stability constant and UV absorption spectrum of the triammine silver(I) complex, *Acta Chemica Scandinavica, series A* 40, 392.
- Bodor, A., Bányai, I., Kowalewski, J. & Glaser, J. 2002. Thallium(III) coordination compounds: chemical information from 205-Tl longitudinal relaxation times, *Magnetic Resonance in Chemistry* 40, 716-722, and references therein.
- Boese, A.D., Chandra, A., Martin, J.M.L. & Marx, D. 2003. From *ab initio* quantum chemistry to molecular dynamics: The delicate case of hydrogen bonding in ammonia, *Journal of Chemical Physics* 119, 5965-5980.
- Bruker. 1995. Bruker SMART and SAINT, area detector control and integration software, Bruker Analytical X-ray systems.
- Burges, C.-W., Koschmieder, R., Sahn, W. & Schwenk, A. 1973. ¹⁰⁷Ag and ¹⁰⁹Ag nuclear magnetic resonance studies of Ag⁺ ions in aqueous solutions, *Zeitschrift für Naturforschung* 28a, 1753-1758.
- Corrosion Doctors site, designed and maintained by KTS. <http://www.corrosion-doctors.org/ProcessIndustry/Process-chemicals.htm> (accessed 5-Jan-2005).
- Department for Environment, Food & Rural Affairs, <http://www.defra.gov.uk/>

- environment/airquality/ammonia/pdf/ammonia_summary.pdf, pp. 1-8 (Accessed 19-Feb-2005).
- Distler, T. & Vaughan, P.A. 1967. The crystal structures of the hexaamminecopper(II) halides, *Inorganic Chemistry* 6, 126-129.
- Factsheets on Chemical and Biological Warfare Agents, Version 2.1, September 2002, <http://www.cbwinfo.com/Chemical/Precursors/Phosphites.html>. (accessed 7-Dec-2004). Freetemplate. <http://www.freetemplate.ws/am/ammonia.html>; (accessed 25-Jan-2005)
- Gans, P. & Gill, J.B. 1976. Spectrochemistry of solutions. Part II. Raman spectra of aqueous and liquid ammonia solutions of metal salts., *Journal of the Chemical Society, Dalton Transactions*, 779.
- Gardiner, D.J., Haji, A.H. & Straughan, B. 1978. Solvation of mercury(II) halides and alkylmercury(II) halides by liquid ammonia: a Raman spectroscopic study, *Journal of the Chemical Society, Dalton Transactions*, 705-710.
- George, G.N. & Pickering, I.J. 1993. EXAFSPAK - A suite of computer programs for analysis of X-ray absorption spectra.
- Gill, D.S., Rodehüser, L., Rubini, P. & Delpuech, J.-J. 1990. Solvation of copper(I) perchlorate in mixed solvent systems containing acetonitrile, *Journal of the Chemical Society. Faraday Transactions* 86, 2847-2852.
- Greenwood, N.N. & Earnshaw, A. 1997. *Chemistry of the Elements*. Pergamon Press, Oxford and references therein.
- Gutmann, V. & Wychera, E. 1966. Coordination reactions in non-aqueous solutions – The role of the donor strength, *Inorganic and Nuclear Chemistry Letters* 2, 257-260.
- Hardy, E.H. & Zeidler, M.D. 2000. The deuterium quadrupole coupling constant in liquid ammonia, *Physical Chemistry Chemical Physics* 2, 1645-1648.
- Hemmerich, P. & Sigwart, C. 1963. Cu(CH₃CN), ein Mittel zum Studium homogener Reaktionen des einwertigen Kupfers in wässriger Lösung, *Experientia* 19, 488-489.
- Hertzberg, G. 1950. *Molecular spectra and molecular structure. Infrared spectra of diatomic molecules*. van Nostrand Co., New York, NY.
- Hillebrecht, H., Thiele, G., Koppenhoefer, A. & Vahrenkamp, H. 1994. Crystal-structure and vibrational-spectra of Zn(NH₃)₄(ClO₄)₂, *Zeitschrift für Naturforschung. Teil B* 49, 1163-1168.
- Holm, R.H., Kennepohl, P. & Solomon, E.I. 1996. Structural and functional aspects of metal sites in biology., *Chemical Reviews* 96, 2239-2314.
- Howarth, O. 1987. *Relaxation and Related Time-Dependent Processes*, ed. J. Mason, Plenum Press, New York, p. 133-170.
- Huheey, J.E., Keiter, E.A. & Keiter, R.L. 1993. *Inorganic Chemistry: Principles of Structure and Reactivity*. HarperCollins, New York.
- Index Mundi, http://www.indexmundi.com/en/commodities/minerals/nitrogen/nitrogen_table12.html (accessed 30-Dec-2004)
- ICSD, Inorganic Crystal Structure Data Base, National Institute of Standards and Technology, Fachinformationszentrum, Karlsruhe, Release 04/1.
- IUPAC Stability Constants Database, Academic Software. 2000. Sourby Old Farm, Otley, Yorks, LS21 2PW, UK.
- Jahlilevand, F. 2000. *Structure of hydrated ions and cyano complexes by X-ray absorption spectroscopy, Thesis*. Royal Institute of Technology, Stockholm, ISBN 91 7170-561-9.
- Jahn, H.A. & Teller, E. 1937. Stability of polyatomic molecules in degenerate electronic states. I. Orbital degeneracy, *Proceedings of the Royal Society of London, Series A Mathematical and Physical Sciences*, 161, 220.
- Johansson, G. 1992. Structures from complexes in solution derived from X-ray diffraction measurements, *Advances in Inorganic Chemistry* 39, 159-233.
- Jolly, W. 1991. *Modern Inorganic Chemistry*.
- Jolly, W.L. & Hallada, C.J. 1965. *Non-aqueous Solvent Systems*. Academic, London.

- Jolly, W.M. 1959. Metal-ammonia solutions, *Progress in Inorganic Chemistry* 1, 235-281.
- Kickelbick, G. & Schubert, U. 1997. ClMPH_3 and $[\text{MPH}_3]^+$ (M=Cu, Ag, Au); a density functional study, *Inorganica Chimica Acta* 262, 61-64.
- Kraus, C.A. 1908. Solution of metals in non-metallic solvents; II. On the formation of compounds between metals and ammonia. *Journal of the American Chemical Society* 30, 653-668.
- Kruh, R.F. & Petz, J.I. 1964. Determination of the structure of liquid ammonia by X-ray diffraction, *The Journal of Chemical Physics* 41, 890-891.
- Kume, T., Sasaki, S. & Shimizu, H. 2001. Raman study of solid ammonia at high pressures and low temperatures, *Journal of Raman Spectroscopy* 32, 383-387.
- Lamble, G., Moen, A. & Nicholson, D. 1994. Structure of the diamminecopper(I) ion in solution. An X-ray absorption spectroscopic study, *Journal of the Chemical Society, Faraday transactions* 90, 2211-2213.
- Lee, H.-G., Matsumoto, Y., Yamaguchi, T. & Othaki, H. 1983. X-Ray Diffraction Studies on the Structures of Hydrated Oxonium Ion, and the Chlorocobalt(II) and Tetrachlorocobaltate(II) Complexes in Aqueous Solution, *Bulletin of the Chemical Society of Japan* 56, 443.
- Liu, Y. & Tuckerman, M.E. 2001. Protonic defects in hydrogen bonded liquids: Structure and dynamics in ammonia and comparison with water, *The Journal of Physical Chemistry B* 105, 6598-6610.
- MacGillavry, C.H. & Bijvoet, J.M. 1936. Die Kristallstruktur der Cadmium- und Quecksilber-Diammin-Dihalogenide, *Zeitschrift für Kristallographie, Kristallgeometrie, Kristallphysik, Kristallchemie* 94, 231-245.
- Maeda, M., Maegawa, Y., Yamaguchi, T. & Othaki, H. 1979. X-ray diffraction studies on the structures of diammine- and aquasilver(I) complexes in aqueous solution, *Bulletin of the Chemical Society of Japan* 52, 2545.
- Makhmudova, N.K., Sharipov, K.T., Khodashova, T.S., Porai-Koshits, M.A. & Parpiev, N.A. 1985. *Doklady Akademii Nauk* 280, 1360.
- Maliarik, M. & Persson, I. Submitted to *Magnetic Resonance in Chemistry*.
- Martan, H. & Weiss, J. 1984. Metall-Schwefelstickstoff-Verbindungen. 17. Die Verbindungen HgN_2S NH_3 und $2\text{Hg}(\text{NH}_3)_2\text{I}_2 \cdot \text{S}_4\text{N}_4$, *Zeitschrift für Anorganische und Allgemeine Chemie* 515, 225-229.
- Massa, W. 2000. *Crystal Structure Determination*. Springer-Verlag, Berlin Heidelberg.
- Maurer, H.M. & Weiss, A. 1977. The crystal structure of diamminesilver dinitroargentate, $[\text{Ag}(\text{NH}_3)_2]\text{Ag}(\text{NO}_2)_2$, *Zeitschrift für Kristallographie* 146, 227.
- Mingos, D.M.P., Yau, J., Menzer, S. & Williams, D.J. 1995. Synthesis of $[\text{Au}(\text{NH}_3)_2]^+$ Salts and the Crystal Structure of $[\text{Au}(\text{NH}_3)_2]\text{Br}$, *Journal of the Chemical Society, Dalton Transactions*, 319-320.
- Mink, J., Németh, C., Hajba, L., Sandström, M. & Goggin, P.L. 2003. Infrared and Raman spectroscopic and theoretical studies of hexaaqua metal ions in aqueous solution, *Journal of Molecular Structure* 661-662, 141-151.
- Moreno, S.D. 1998. *Estudio de la estructura de complejos metálicos en disolución mediante espectroscopías de absorción de rayos X, On the structures of mercury(II) halide complexes and the solvation of mercury(II), cadmium(II) and zinc(II) in solution and in crystals, determined by X-ray diffraction and spectroscopic methods*, Thesis. Universidad de Sevilla, Sevilla.
- Nakamoto, K. 1997. *Infrared and Raman Spectra of Inorganic and Coordination Compounds*. Wiley-Interscience, New York.
- Narten, A.H. 1977. Liquid ammonia: Molecular correlation functions from X-ray diffraction, *Journal of Chemical Physics* 66, 3117-3120.

- Nockemann, P. & Meyer, G. 2002. $[\text{Ag}(\text{NH}_3)_2]\text{ClO}_4$: Kristallstrukturen, Phasenumwandlung, Schwingungsspektren, *Zeitschrift für Anorganische und Allgemeine Chemie* 628, 1636-1640.
- Nockemann, P. & Meyer, G. 2003. Zwei Mercuri-Ammin-Komplexe: $[\text{Hg}(\text{NH}_3)_2][\text{HgCl}_2]_2$ und $[\text{Hg}(\text{NH}_3)_4](\text{ClO}_4)_2$, *Zeitschrift für Anorganische und Allgemeine Chemie* 629, 123-128.
- Occupational Safety & Health Administration U. S. Department of Labor
<http://www.osha.gov/SLTC/healthguidelines/trimethylphosphite/> (accessed 7-Dec-2004)
- Ohtaki, H. & Radnai, T. 1993. Structure and dynamics of hydrated ions, *Chemical Reviews* 93, 1157-1204, and references therein.
- Olovsson, I. & Templeton, D.H. 1959. X-ray study of solid ammonia, *Acta Crystallographica* 12, 832-837.
- Pearson, R.G. 1963. Hard and soft acids and bases, *Journal of the American Chemical Society* 85, 3533-3539.
- Persson, I., Penner-Hahn, J.E. & Hodgson, K.O. 1993. An EXAFS spectroscopic study of solvates of copper(I) and copper(II) in acetonitrile, dimethyl sulfoxide, pyridine and tetrahydrothiophene solutions and a Large-Angle X-ray Scattering study of the copper(II) acetonitrile solvate in solution, *Inorganic Chemistry* 32, 2497-2501.
- Persson, I., Persson, P., Sandström, M. & Ullström, A.-S. 2002. Structure of Jahn-Teller distorted solvated copper(II) ions in solution, and in solids with apparently regular octahedral coordination geometry, *Journal of the Chemical Society, Dalton Transactions*, 1256-1265.
- Persson, I., Sandström, M., Yokoyama, H. & Chaudhry, M. 1995. Structures of the solvated barium and strontium ions in aqueous, dimethylsulfoxide and pyridine solution, and crystal structure determination of strontium and barium hydroxide octahydrate, *Zeitschrift für Naturforschung, Teil A: Physical Science* 50, 21-37.
- Pranowo, H.D. & Rode, B.M. 1999. Solvation of Cu^{2+} in liquid ammonia: Monte Carlo simulation including three-body corrections, *Journal of Physical Chemistry A* 103, 4298-4302.
- Pykkö, P. 2004. Theoretical chemistry of gold, *Angewandte Chemie. International Edition in English* 43, 4412-4456.
- Raman, C.V. & Krishnan, K.S. 1928. A new type of secondary radiation. *Nature* 121, 501.
- Ricci, M.A., Andreani, C. & Soper, A.K. 1995. Microscopic structure of low temperature liquid ammonia: A neutron diffraction experiment, *Journal of Chemical Physics* 102, 7650-7655.
- Sanders, J.K.M. & Hunter, B.K. 1993. *Modern NMR Spectroscopy*. Oxford University Press, Oxford.
- Sandström, M. 1978. *On the structures of mercury(II) halide complexes and the solvation of mercury(II), cadmium(II) and zinc(II) in solution and in crystals, determined by X-Ray diffraction and spectroscopic methods*, Thesis. Royal Institute of Technology, Stockholm.
- Sandström, M., Persson, I. & Persson, P. 1990. A study of solvent electron-pair donor ability and Lewis basicity scales, *Acta Chemica Scandinavica* 44, 653-675.
- Schwenk, C.F. & Rode, B.M. 2004. Cu(II) in liquid ammonia: An approach by hybrid quantum-mechanical/molecular-mechanical molecular dynamics simulation, *ChemPhysChem* 5, 342-348.
- Schwerdtfeger, P. 2002. Relativistic effects in properties of gold, *Heteroatom Chemistry* 13, 578-584, and references therein.
- Seward, T.M., Henderson, C.M.B., Charnock, J.M. & Dobson, B.R. 1996. An X-ray absorption (EXAFS) spectroscopic study of aquated Ag^+ in hydrothermal solutions to 350°C, *Geochimica Cosmochimica Acta* 60, 2273-2282.
- Shannon, R.D. 1976. Revised effective ionic radii and systematic studies of interatomic distances in halides and chalcogenides, *Acta Crystallographica A* 32, 751.

- Sheldrick, G.M. 1990. Phase annealing in SHELX-90: direct methods for larger structures, *Acta Crystallographica, Section A* 46, 467-473.
- Shipman, L.L., Burgess, A.W. & Scheraga, H.A. 1976. Lattice energies and heats of sublimation at 0 K for *n*-pentane, *n*-hexane, *n*-octane and ammonia, *Journal of Physical Chemistry B* 80, 52.
- Smiechowski, M. & Persson, I. *Unpublished data*.
- Stoe & Cie GmbH, Hilpertstraße 10, D-64295 Darmstadt.
- Stålhandske, C.M.V. 1996. *N,N-Dimethylthioformamide, A structural and spectroscopic study of the solvent and some solvated metal ions and complexes*, Thesis. Uppsala. ISBN 91-576-5216-3.
- Stålhandske, C.M.V., Persson, I., Sandström, M. & Kamienska-Piotrowicz, E. 1997. Structure of the solvated zinc(II), cadmium(II), and mercury(II) ions in *N,N*-dimethylthioformamide solution, *Inorganic Chemistry* 36, 3174.
- Stålhandske, C.M.V., Stålhandske, C.I., Persson, I., Sandström, M. & Jahlilshvand, F. 2001. Crystal and solution structures of *N,N*-dimethylthioformamide-solvated copper(I), silver(I) and gold(I) ions studied by X-ray diffraction, X-ray absorption and vibrational spectroscopy, *Inorganic Chemistry* 40, 6684-6693.
- Suresh, S.J. & Naik, V.M. 2000. Hydrogen bond thermodynamic properties of water from dielectric constant data, *Journal of Chemical Physics* 113, 9727-9732.
- Thompson, H., Wasse, J.C., Skipper, N.T., Hayama, S., Bowron, D.T. & Soper, A.K. 2003. Structural studies of ammonia and metallic lithium-ammonia solutions, *Journal of the American Chemical Society* 125, 2572-2581.
- Thompson, J.C. 1976. *Electrons in Liquid Ammonia*. Clarendon Press, Oxford, U. K.
- Tolman, C.A. 1977. Steric effects of phosphorus ligands in organometallic chemistry and homogeneous catalysis, *Chemical Reviews* 77, 313-348.
- Ujike, T. & Tominaga, T. 2002. Raman spectral analysis of liquid ammonia and aqueous solution of ammonia, *Journal of Raman Spectroscopy* 33, 485-493.
- Valli, M., Matsuo, S., Wakita, H., Yamaguchi, T. & Nomura, M. 1996. Solvation of copper(II) ions in liquid ammonia, *Inorganic Chemistry* 35, 5642-5645.
- Wallinder F. 2004. Mars 2.0, *Forskning & Framsteg* 06/04, 20-23.
- Wasylishen, R.E. 1987. *NMR Relaxation and Dynamics*, Marcell Dekker Inc., New York, p. 54-91.
- Wasse, J.C., Hayama, S., Skipper, N.T., Morrison, D. & Bowron, D.T. 2003. Liquid-liquid phase separation and microscopic structure in rubidium-ammonia solutions observed using X-ray absorption spectroscopy, *Journal of Physical Chemistry B* 107, 14452-14456.
- Wisconsin Department of Health and Family Services, <http://dhfs.wisconsin.gov/eh/Air/fs/Ammonia.htm> (accessed 15-Feb-2005)
- Wernet, P., Nordlund, D., Bergman, U., Cavalleri, M., Odelius, M., Ogasawara, H., Näslund, L.Å., Hirsch, T.K., Ojamäe, L., Galztel, P., Petterson, L.G.M. & Nilsson, A. 2004. The structure of the first coordination shell in liquid water, *Science* 304, 995-999.
- X-ray Absorption Spectroscopy Laboratory – University of Camerino, http://gnxas.unicam.it/XASLABwww/pag_gnxas.html (accessed 15-Feb-2005)
- Yamaguchi, T., Johansson, G., Holmberg, B., Maeda, M. & Ohtaki, H. 1984. The coordination and complex formation of silver(I) in aqueous perchlorates, nitrate and iodide solutions, *Acta Chemica Scandinavica, Series A* 38, 437.
- Yamaguchi, T., Wakita, H. & Nomura, M.J. 1988. Silver(I) solvation in some N-donor solvents from Ag K-edge EXAFS, *Journal of the Chemical Society, Chemical Communications*, 433-434.
- Zabinsky, S.I., Rehr, J.J., Ankudinov, A., Albers, R.C. & Eller, M.J. 1995. FEFF code for ab initio calculations of XAFS, *Physical Reviews B* 52, 2995; A. Ankudinov, The FEFF

- program. 1996, Thesis, University of Washington: Available from <http://Feff.phys.-washington.edu/feff>.
- Zachiweja, U. & Jacobs, H. 1992. Redetermination of the crystal structure of diamminesilver(I) sulfate, $[\text{Ag}(\text{NH}_3)_3]\text{SO}_4$, *Zeitschrift für Kristallographie* 201, 207.
- Zachwieja, U. & Jacobs, H. 1989. Kolumnarstrukturen bei Tri- und Diamminnitraten, $[\text{M}(\text{NH}_3)_3]\text{NO}_3$ und $[\text{M}(\text{NH}_3)_2]\text{NO}_3$ des einwertigen Kupfers und Silbers, *Zeitschrift für Anorganische und Allgemeine Chemie* 571, 37-50.

Appendices

A. Abbreviations

APES	Adiabatic Potential Energy Surface
CSA	Anisotropic Chemical Shielding
DSC	Differential Scanning Calorimetry
DD	Dipole-Dipole
EXAFS	Extended X-ray Absorption Fine Structure
HOMO	Highest Occupied Molecular Orbital
JT	Jahn-Teller
JTE	Jahn-Teller Effect
NMR	Nuclear Magnetic Resonance
LAXS	Large Angle X-ray Scattering
LUMO	Lowest Unoccupied Molecular Orbital
PJT	Pseudo Jahn-Teller
PJTE	Pseudo Jahn-Teller Effect
SC	Scalar Coupling
SR	Spin-Rotation
XAS	X-ray Absorption Spectroscopy

B. Tolman cone angles

The ligand cone angle, θ /°, determined for phosphite and phosphine ligands with Ni(0) as the coordinated metal. (Tolman, 1977)

Type of ligand	PR_3	$\text{P}(\text{OR})_3$	θ
		$\text{P}(\text{OCH}_3)_3$	107
		$\text{P}(\text{OC}_2\text{H}_5)_3$	109
	$\text{P}(\text{CH}_3)_3$		118
		$\text{P}(\text{OC}_6\text{H}_5)_3$	128
		$\text{P}(\text{O-}i\text{-C}_3\text{H}_7)_3$	130
	$\text{P}(\text{C}_2\text{H}_5)_3$		132
	$\text{P}(\text{C}_4\text{H}_{10})_3$		132
	$\text{P}(\text{C}_6\text{H}_5)_3$		145